



### 저작자표시-비영리-변경금지 2.0 대한민국

이용자는 아래의 조건을 따르는 경우에 한하여 자유롭게

- 이 저작물을 복제, 배포, 전송, 전시, 공연 및 방송할 수 있습니다.

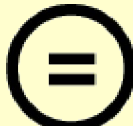
다음과 같은 조건을 따라야 합니다:



저작자표시. 귀하는 원 저작자를 표시하여야 합니다.



비영리. 귀하는 이 저작물을 영리 목적으로 이용할 수 없습니다.



변경금지. 귀하는 이 저작물을 개작, 변형 또는 가공할 수 없습니다.

- 귀하는, 이 저작물의 재이용이나 배포의 경우, 이 저작물에 적용된 이용허락조건을 명확하게 나타내어야 합니다.
- 저작권자로부터 별도의 허가를 받으면 이러한 조건들은 적용되지 않습니다.

저작권법에 따른 이용자의 권리와 책임은 위의 내용에 의하여 영향을 받지 않습니다.

이것은 [이용허락규약\(Legal Code\)](#)을 이해하기 쉽게 요약한 것입니다.

[Disclaimer](#)



# **The role of the unfolded protein response in noise-induced hearing loss and the identification of therapeutic targets**

**Ji Won Hong**

**The Graduate School  
Yonsei University  
Department of Medical Science**

# **The role of the unfolded protein response in noise-induced hearing loss and the identification of therapeutic targets**

**A Dissertation Submitted  
to the Department of Medical Science  
and the Graduate School of Yonsei University  
in partial fulfillment of the  
requirements for the degree of  
Doctor of Philosophy in Medical Science**

**Ji Won Hong**

**January 2025**



**This certifies that the Doctoral Dissertation  
of Ji Won Hong is approved.**

2028

Thesis Supervisor Heon Yung Gee

Thesis Committee Member Jinwoong Bok

Thesis Committee Member Chul Hoon Kim

Thesis Committee Member Jinsei Jung

Thesis Committee Member Byung Yoon Choi

**The Graduate School  
Yonsei University  
June 2024**

## ACKNOWLEDGEMENTS

끝이 보이지 않던 학위 과정도 끝이 나네요. 처음 박사과정으로 입학하여 고군분투했을 때가 엊그제 같은데 졸업이 아직 실감이 나지 않습니다. 입학했을 때 저는 많이 부족한 사람이었는데 지현영 교수님지도 아래 많은 것을 배우고 다양한 것을 경험하며 한층 더 성장할 수 있었습니다. 박사 학위 과정 동안 지현영 교수님의 지도를 받을 수 있어서 행운이었다고 생각하고 교수님께 부끄러운 제자가 되지 않도록 어디에서든 열심히 연구에 정진하며 연구의 뜻을 이어가도록 하겠습니다. 학위 과정 동안 부족한 저를 믿고 연구를 이어갈 수 있도록 지도해 주신 지현영 교수님께 감사의 말씀을 올립니다.

감사하게도 박사 학위 과정 동안 많은 분들이 도움을 주셨습니다. 먼저 지도교수가 아님에도 제 연구에 관심을 가져 주시고 매번 진정성 있는 디스커션으로 연구를 더 나은 방향으로 이끌어주신 복진웅 교수님, 김철훈 교수님, 정진세 교수님, 최병윤 교수님께 감사의 말씀을 드립니다. 그리고 해당 분야 실험에 대해 매번 많은 도움을 주신 복진웅 교수님 연구실의 민혜현 박사님께도 감사하다는 말씀을 전하고 싶습니다. 2019년 8월 제가 처음 실험실에 왔을 때 적응할 수 있도록 도와주고 매번 친절하게 도움을 준 세영이, 김혜연 박사님, 고영익 박사님께 감사 인사를 드리며 옆에 앉아 힘들 때 의지가 된 선영이, 입학 동기로 의지를 많이 했던 경석이, 힘든 실험실 생활에 항상 웃음을 줬던 정아, 즐거운 시간 보냈던 유진, 소연이, 뒤에 앉아 응원해 준 오종욱 선생님, 긍정적인 에너지를 줬던 이동기, 노재원, 장승현 선생님, 착한 세진이, 사람 좋은 형기, 속이 깊은 우철이를 포함하여 제 학위 기간 중 도움을 주신 많은 분들께 감사하다는 말 전하고 싶습니다. 좋은 사람들을 만나 힘든 학위 기간이 마냥 힘들게만 느껴지지 않았던 것 같습니다.

마지막으로 학부 졸업 후 박사 졸업까지 긴 여정을 뒤에서 묵묵히 저를 응원해 주시고 가장 큰 힘이 되어준 우리 엄마, 아빠에게 존경하고 감사하다는 말씀을 전합니다. 엄마, 아빠의 사랑과 정성으로 제가 여기까지 올 수 있었고 앞으로 살아갈 많은 날들, 보답하면서 살아가겠습니다.

그리고 우리 언니, 형부, 지아, 재현이, 인생의 질반을 함께한 친구들, 사랑하는 우리 고양이 레오에게도 옆에서 힘이 돼 주어서 고맙다는 말을 전하고 싶습니다.

2024.06

## TABLE OF CONTENTS

LIST OF FIGURES .....	ii
ABSTRACT IN ENGLISH .....	iv
1. INTRODUCTION .....	1
2. MATERIALS AND METHODS .....	2
2.1. Mice .....	2
2.2. Noise exposure .....	2
2.3. Auditory Brainstem Response (ABR) and Distortion Product Otoacoustic Emissions (DPOAE) .....	2
2.4. RNA-sequencing and bioinformatics analyses .....	3
2.5. Western blotting .....	4
2.6. Immunofluorescence .....	4
2.7. Pharmacological modulation of UPR by intraperitoneal injection .....	5
2.8. Scanning electron microscopy .....	6
2.9. Statistical data analysis .....	6
3. RESULTS .....	7
3.1. Noise exposure induces longitudinal alterations in the cochlear transcriptome .....	7
3.2. Noise exposure inducing TTS and PTS triggers ER stress and unfolded protein response .....	18
3.3. The protein kinase R-like endoplasmic reticulum kinase (PERK) branch of UPR is continuously activated in response to PTS-inducing noise .....	26
3.4. Inhibition of PERK activity before and after TTS-inducing noise exposure interferes with hearing recovery .....	31
3.5. The inhibition of persistent activation of PERK mitigates noise-induced hearing loss ..	35
3.6. Administration of pharmacological chaperones immediately after noise exposure protects noise-induced hearing loss .....	38
3.7. Pharmacological chaperones suppress the expression of CHOP and aggresomes in hair cells following noise exposure .....	41
4. DISCUSSION .....	46
5. CONCLUSION .....	49
REFERENCES .....	50
ABSTRACT IN KOREAN .....	56

## LIST OF FIGURES

<Fig 1> Schematic representation of the experimental design .....	9
<Fig 2> Exposure to TTS-inducing noise results in hearing recovery after 2 weeks, whereas exposure to PTS-inducing noise leads to permanent hearing loss .....	10
<Fig 3> Exposure to PTS-inducing noise impedes the recovery of click and wave I amplitudes .....	11
<Fig 4> Scanning Electron Microscope (SEM) images of the adult mouse cochlea after TTS and PTS-inducing noise exposure up to 2 weeks .....	12
<Fig 5> Box plot and correlation matrix for RNA-sequencing in the cochlea after noise exposure ..	13
<Fig 6> Principal Component Analysis (PCA) plots of cochlear transcriptome data over time following TTS and PTS-induced noise exposure .....	14
<Fig 7> Heatmap of Differentially Expressed Genes (DEGs) in samples exposed to TTS and PTS-induced noise exposure .....	15
<Fig 8> Manhattan plot of Gene Ontology (GO) enrichment analysis results for all clusters of Differentially Expressed Genes (DEGs) .....	16
<Fig 9> Bar charts for the Gene Ontology (GO) analysis of DEGs .....	17
<Fig 10> Pie charts and bar charts representing the Reactome and Enrichr pathway analysis of DEGs .....	20
<Fig 11> Immune cell deconvolution analysis based on RNA sequencing .....	21
<Fig 12> Exposure to TTS and PTS-induced noise triggers ER stress and UPR in the cochlea .....	22
<Fig 13> Expression of ER stress and UPR-related factors in each cell type of cochlea 1 day after exposure to PTS-inducing noise .....	23
<Fig 14> Exposure to TTS and PTS-induced noise induces aggresome formation in cochlear .....	24
<Fig 15> The PERK branch remains continuously activated up to 2 weeks following PTS-induced noise exposure .....	28
<Fig 16> PTS-induced noise exposure induces the expression of CHOP in the hair cells of the cochlea .....	29
<Fig 17> Scanning Electron Microscope (SEM) images of adult mouse cochlea after 4 weeks of TTS- and PTS-inducing noise exposure .....	30
<Fig 18> Treatment with the PERK inhibitor, GSK2656157 before and after exposure to TTS-inducing noise leads to a decrease in p-PERK expression .....	32
<Fig 19> Inhibition of PERK early after TTS-inducing noise exposure disrupts hearing recovery ..	33
<Fig 20> The initial inhibition of PERK activity following PTS-inducing noise exposure does not	

affect in hearing recovery.....	34
<Fig 21> Inhibition of sustained activation of PERK following PTS-inducing noise exposure is beneficial for hearing recovery.....	36
<Fig 22> A strategy for treating noise-induced hearing loss using pharmacological chaperones .....	39
<Fig 23> Pharmacological chaperones have protective effects against hearing loss induced by permanent threshold shift (PTS)-inducing noise exposure .....	40
<Fig 24> Pharmacological chaperones inhibit the expression of CHOP in the hair cells of the cochlea after PTS-inducing noise exposure .....	42
<Fig 25> Pharmacological chaperones inhibit the accumulation of aggresome in the hair cells of the cochlea after PTS-inducing noise exposure .....	44
<Fig 26> Graphical summary of unfolded protein response (UPR) activation in the cochlea over time following TTS and PTS-inducing noise exposure.....	45

## ABSTRACT

### **The role of the unfolded protein response in noise-induced hearing loss and the identification of therapeutic targets**

Noise-induced hearing loss can be temporary (transient threshold shift, TTS) or permanent (permanent threshold shift, PTS), depending on the intensity and duration of exposure. Prolonged exposure to excessive noise activates various cellular mechanisms within the cochlea, such as oxidative stress, immune response, and apoptosis. Currently, no study has thoroughly investigated the temporal alterations of cochlear transcriptome following exposure to temporary threshold shift (TTS)- or permanent threshold shift (PTS)-inducing noise to identify pathogenic mechanisms and therapeutic targets for noise-induced hearing loss. We analyzed the longitudinal alterations in the cochlear transcriptome of adult mice exposed to noise in two distinct conditions, revealing variations in hearing recovery. We found that endoplasmic reticulum stress induced by noise exposure activated the unfolded protein response (UPR), specifically activating inositol-requiring enzyme type 1 $\alpha$  (IRE1 $\alpha$ ) and protein kinase R-like endoplasmic reticulum kinase (PERK) among the three UPR branches. Additionally, the PERK branch exhibited sustained activation in the permanent threshold shift (PTS) up to 2 weeks after noise exposure, but it returned to baseline levels in the transient threshold shift (TTS). The pro-apoptotic factor CHOP, subfactor of the PERK branch, was significantly induced in hair cells during PTS. However, treatment with a PERK inhibitor before noise exposure did not restore hearing, indicating that PERK activation is necessary for hearing recovery. Interestingly, pharmacological chaperone treatments such as tauroursodeoxycholic acid (TUDCA) and 4-phenylbutyric acid (4-PBA) have achieved hearing protection even in cases of noise-induced permanent threshold shift (PTS). Overall, PERK branch of the unfolded protein

response is closely associated with the mechanism of NIHL. Initial activation of PERK is necessary for hearing recovery after noise exposure, while persistent activation hinders hearing recovery. Furthermore, the hearing recovery effect of pharmacological chaperones suggests a new therapeutic target in NIHL that was previously unknown.

---

Key words : Noise-induced hearing loss; RNA-sequncing; Endoplasmic reticulum stress; Unfolded protein response; PERK; CHOP; Pharmacological chaperone; TUDCA; 4-PBA

## 1. Introduction

Noise-induced hearing loss (NIHL) is a significant global health concern that is rapidly increasing due to exposure to occupational and environmental noise. According to the World Health Organization (WHO), one out of three instances of hearing impairment is linked to noise exposure, putting over 1 billion individuals aged 12 to young adults worldwide at risk of noise-induced hearing loss.<sup>1-3</sup>

The cochlea, a spiral-shaped structure situated in the inner ear, is tonotopically arranged along its axis, playing a vital role in transforming sound vibrations into electrical signals and transmitting them to the brain.<sup>4</sup> The intricate cellular structure known as the organ of Corti, located within the cochlea, contains a single row of inner hair cells (IHCs) and three rows of outer hair cells (OHCs). OHCs amplify sound vibrations and transmit them to the auditory cortex of the brain through the auditory nerve fibers (ANFs) associated with IHCs, allowing us to perceive sound.<sup>5-9</sup>

The noise causing noise-induced hearing loss (NIHL) is classified into Temporary Threshold Shift (TTS), where the hearing threshold changes temporarily, and Permanent Threshold Shift (PTS), where the changes are permanent, based on intensity and duration of the noise. Noise that induces TTS is commonly encountered in daily life, causing a temporary increase in the hearing threshold that recovers to the basal level over time. In contrast, exposure to noise that induces PTS results in a sudden and irreversible increase in the hearing threshold, leading to non-recoverable changes in hearing and adversely affecting the quality of life.<sup>10-12</sup> The noise that causes PTS has been shown to result in structural collapse like the abnormalities of stereocilia<sup>13</sup>, loss of OHCs<sup>14-15</sup>, and fusion of IHCs.<sup>16</sup> Additionally, noise inducing PTS stimulates processes such as apoptosis<sup>17</sup>, autophagy<sup>15</sup>, inflammation<sup>18-20</sup>, oxidative stress<sup>21-23</sup>, calcium overload<sup>24-25</sup>, and glutamate excitotoxicity.<sup>26</sup> PTS-inducing noise might also increase the production of lipid peroxidation products and decrease blood flow in the cochlea.<sup>27</sup>

In recent RiboTag and single-cell RNA sequencing, an immediate upregulation of immune-related genes, along with transcription factors STAT3 and IRF7, was observed in nearly all cell types following noise exposure.<sup>28</sup> Unlike PTS, TTS-inducing noise stimuli do not result in OHC loss even over time after noise exposure.<sup>15</sup> As far as currently known, it only causes damage to stereocilia and a reduction in ribbon synapses.<sup>29</sup> In a recent study, the proteome in the cochlea was compared and analyzed immediately after exposure to TTS- and PTS-inducing noise and two weeks later. The

findings suggest the potential role of the protein translation machinery in hearing recovery.<sup>29</sup> Nevertheless, the mechanisms of hearing recovery and therapeutic targets for noise-induced hearing loss are not clear. This study investigated longitudinal changes in the mouse cochlear transcriptome following TTS- and PTS-inducing noise stimuli using RNA-sequencing. Additionally, we identified therapeutic targets based on the longitudinal analysis and investigated the effects of pharmacological intervention on noise-induced hearing loss, as well as its preventive capabilities.

## 2. Materials and Methods

### 2.1 Mice

C57BL/6N mice were purchased from Orient Bio (Seongnam, Korea). After transportation, all the mice were allowed to acclimatise for one week. The animal experimental protocols were reviewed and approved by the Institutional Animal Care and Use Committee of Yonsei University College of Medicine. All mice were handled in accordance with the Guidelines for the Care and Use of Laboratory Animals. Mice were maintained in a temperature- and humidity-controlled, specific pathogen-free (SPF) environment with a light cycle from 8:00 AM to 8:00 PM and unlimited access to water and irradiated rodent food (LabDiet, 0006972).

### 2.2 Noise exposure

C57BL/6N mice at the age of 8 weeks were exposed to 105 dB SPL for 1 hour to induce TTS and to 110 dB SPL for 2 hours to induce PTS. The mice were placed in a circular wire mesh exposure cage with eight compartments inside a soundproof booth. Noise signals were transmitted from a computer through an amplifier (INTER-M R300 Plus power amplifier; Canford Audio PLC, Washington, UK) to a loudspeaker (ElectroVoice DH1A-WP; Sonic Electronix, Inc., Los Angeles, CA, USA). The noise level was measured using a 1/2-inch Electret condenser microphone (TES-1350A).

### 2.3 ABR and DPOAE

To measure ABR and DPOAE, the mice were anesthetized via intraperitoneal injection of 10

mg/kg xylazine (Rompun, Bayer Animal Health, Monheim, Germany) and 40 mg/kg zolazepam HCl (Zoletil, Virbac Animal Health, Carros, France). ABR thresholds were assessed with the TDT System-3 (Tucker Davis Technologies, Gainesville, FL, USA) before noise exposure and at 2 hours, 1 day, and 14 days post-exposure to TTS- or PTS-inducing noise. Subcutaneous needle electrodes were placed around the infra-auricular regions and the skull vertex. Calibrated click stimuli (10  $\mu$ s duration) or tone burst stimuli (5 ms duration) at 6, 8, 12, 18, 24, and 30 kHz were generated using SigGenRZ software and the RZ6 digital signal processor, and delivered to the ear canal via a multi-field 1 (MF1) magnetic speaker (TDT). Stimulus intensity ranged from 10 to 90 dB SPL in 5 dB increments. The ABR signals were captured by a low-impedance Medusa Biological Amplifier System (RA4LI, TDT), processed by the RZ6 digital signal-processing hardware, filtered with a 0.5–1 kHz band-pass filter, and averaged over responses to 256 tone bursts. The DPOAE was measured with a TDT microphone-speaker system. Stimulus tones were generated by the RZ6 digital signal processor with SigGenRZ software and delivered via a custom probe with an ER 10B+ microphone (Etymotic, Elk Grove Village, IL, USA) and an MF1 speaker in the ear canal. Primary tones were set at a frequency ratio (f<sub>2</sub>/f<sub>1</sub>) of 1.2 with target frequencies of 6, 8, 12, 18, 24, and 30 kHz, and f<sub>2</sub> intensity equal to f<sub>1</sub> intensity (L<sub>1</sub> = L<sub>2</sub>). An ER 10B+ microphone captured the primary tones, recorded by the RZ6 digital signal processor. The DPOAE input/output (I/O) function was determined at specific frequencies (6 to 30 kHz) with a frequency ratio (f<sub>2</sub>/f<sub>1</sub>) of 1.2 and equal intensities (L<sub>1</sub> = L<sub>2</sub>). Primary tone intensity increased from 20 to 80 dB SPL in 5 dB increments. The average spectra of the primary tones, 2f<sub>1</sub>-f<sub>2</sub> distortion products, and noise floors were determined using BioSigRZ's Fast Fourier transform (FFT) for each primary tone and intensity.

## 2.4 RNA-sequencing and bioinformatics analyses

Total RNA from the cochlea was extracted using TRIzol, following the manufacturer's protocol, and then purified using an RNeasy Plus Mini kit (QIAGEN). Quality control reagents and libraries were created according to Macrogen's (Seoul, Korea) standard procedure for gene expression analysis. Libraries were sequenced using an Illumina NovaSeq 6000 sequencing system. CLC Genomics Workbench 9.5.3 software (Qiagen) was used to map the reads to the mouse genome (mm10, build name GRCm38) and generate gene expression values in the normalised form of TPM values. All differentially expressed genes (DEGs) were chosen using analysis of variance (ANOVA)

( $P < 0.05$ , absolute 1.5-fold change, and TPM > 1). We visualised the RNA-seq analysis including hierarchical clustering heatmaps and principal component analysis, and the bar graph of GO results using R studio v3.6.3. Functional enrichment with Gene ontology was performed using g:Profiler 2, Enrichr, and Gene Set Enrichment Analysis (GSEA) v4.1.0 was performed using Hallmark gene sets from the Molecular Signatures Database (MSigDB).

## 2.5 Western blotting

The dissected cochlear tissue was homogenised in a lysis buffer containing a protease and phosphatase inhibitor cocktail (Thermo Scientific, cat. 78440). Four cochlear tissues (two mice) were used for each western blot sample. Lysates were then incubated on ice for 10 min before sonication using a QSonica Q700 Sonicator (M2 Scientific, cat Q700) with an amplitude set to 20 for 30 s. The lysates were centrifuged for 20 min at 15,000 rpm at 4 °C, and the supernatants were collected. Protein concentrations were measured using the Protein Assay Dye Reagent (Bio-Rad, cat. 5000006). Samples for electrophoresis were prepared by adding 5X SDS loading buffer to 40 µg of cochlear lysates and boiled at 100 °C for 10 min. SDS-PAGE was run on 4–15% gradient mini-protein TGX gels (Bio-Rad) and proteins were transferred to nitrocellulose membranes using the Bio-Rad Trans-Blot Turbo transfer system (250 mA-100 minutes). The membranes were blocked with a 5% blocking reagent (Biopure, cat. 8110s) for 1 hour at room temperature, followed by an overnight incubation at 4 °C with the primary antibody at a 1:1000 dilution. The membranes were then washed three times with TBST and incubated with anti-rabbit IgG-HRP (Enzo, cat# ADI-SAB-300-J) or anti-mouse IgG-HRP (Enzo, cat# ADI-SAB-100-J) secondary antibodies (1:1000) for 1 h at room temperature. After washing with TBST, antibody-antigen complexes were captured using SuperSignal West Femto chemiluminescent substrates (Thermo, cat# 34096) and bands were detected using the ImageQuant 800 System (Cytiva, Korea). The following primary antibodies were used: PDI (Cell signalling, SC3501T), BIP (Abcam, ab21685), p-PERK (Sigma, PA5-102853), PERK (Cell signalling, SC5683), p-IRE1α (Abcam, ab124945), IRE1α (Cell signalling, SC3294T), CHOP (Cell signalling, T2895S), cleaved-ATF6 and ATF6 (Novus, NBPI-40256), and β-actin (Cell signalling, SC3700). Protein bands were quantified using ImageJ software.

## 2.6 Immunofluorescence

Inner ears were dissected in phosphate-buffered saline (PBS) and fixed overnight at 4 °C in 4% paraformaldehyde (PFA). The samples were decalcified by incubation in 0.5 M EDTA for 1 d at 4 °C. The cochlea was separated from the epithelium and tectorial membrane, microdissected, and fixed in 4% paraformaldehyde for 1 h at 4 °C. The fixed cochleae were blocked and permeabilised with 10% goat serum in 0.5% Triton X-100 for 1 h at room temperature. These samples were incubated overnight at 4 °C with the primary antibody (1:500) (CHOP, Cell signal, T2895S) diluted with 3% goat serum in 0.5% Triton X-100 with gentle agitation. After washing thrice with 1X PBS, the samples were incubated with Alexa Fluor 488-conjugated secondary antibodies (1:500) (Thermo Fisher Scientific, Rockford, IL, USA) diluted in 3% goat serum in 0.5% Triton X-100 at room temperature for 90 min. The samples were then counterstained with DAPI and Alexa Fluor-conjugated Phalloidin 594 (Thermo Fisher Scientific, Rockford, IL, USA). The cells were washed thrice with 1x PBS and mounted on a glass slide with ProLong Gold anti-fade reagent (Thermo Fisher Scientific, Rockford, IL, USA), and imaged using an LSM 780 confocal microscope (Carl Zeiss, Jena, Germany). The images were processed using ZEN (Blue edition) software. Aggresome staining (PROTEOSTAT Aggresome Detection Kit; Enzo Life Sciences) was performed according to the manufacturer's recommendations.

## 2.7 Pharmacological modulation of UPR by intraperitoneal injection

The PERK inhibitor GSK2656157 (Selleck Chem, S7033) was dissolved in dimethyl sulfoxide (DMSO) as a 25 mg/ml stock solution. The GSK2656157 stock solution was diluted in 10% DMSO before use. Mice in the PERK inhibitor treatment group were intraperitoneally injected with a final dose of 40 mg/kg for a total of five times up to 3 days immediately before and after the TTS-inducing noise exposure. Two types of chemical chaperones, 4-phenylbutyric acid (4-PBA) (Medchem, HY-A0281) and sodium taurooursodeoxycholate (TUDCA) (Millipore, 14605-22-2) were used. Further, 100 mg/ml 4-PBA was dissolved in DMSO as a stock solution. Before use, the 4-PBA stock solution was diluted to the total volume in 1X PBS containing 10% DMSO. TUDCA was dissolved in filtered 1X PBS as a 100 mg/ml stock solution. Before treatment, the TUDCA stock solution was diluted with 1X PBS to the same volume as 4-PBA. Chemical chaperones were intraperitoneally injected at a dose of 300 mg/kg daily for up to 2 weeks, immediately after exposure to PTS-inducing noise. Control mice were injected with the same volume of vehicle solution.

## 2.8 Scanning electron microscopy

Cochlear tissues were dissected and fixed overnight at 4 °C in Karnovsky's fixative (2% Glutaraldehyde, 2% paraformaldehyde in 0.1M phosphate buffer, pH 7.4). Cochleae were decalcified overnight at 4 °C with 0.5 M EDTA solution. After decalcification, the cochlear epithelium and tectorial membrane were separated and fixed overnight at 4 °C with Karnovsky's fixative. The fixed samples were washed thrice in 0.1 M phosphate buffer. Post-fixing was performed in 1% OsO<sub>4</sub> (Polysciences, Cat# 02236) for 2 hours followed by dehydration with an increasing ethanol gradient (50–100%), and critical point drying (LEICA EM CPD300). The samples were then coated with platinum by ion sputtering (LEICA EM ACE600) and observed using a field-emission scanning electron microscope (MERLIN, ZEISS).

## 2.9 Statistical analysis

Statistical analyses were conducted using PRISM 8.0 (GraphPad, San Diego, CA, USA). All graphed results are expressed as means  $\pm$  S.E.M. Statistical comparisons were made using two-way analysis of variance (ANOVA) with Bonferroni's corrections for multiple comparisons. Statistical significance is indicated in the figures as n.s., non-significant ( $P > 0.05$ ),  $*P < 0.05$ ,  $**P < 0.01$ , and  $***P < 0.001$ . All other analyses were conducted with at least three independent experiments or samples to minimise statistical errors.

### 3. Results

#### 3.1 Noise exposure induces longitudinal alterations in the cochlear transcriptome

To explore the temporal alterations in the transcriptome and distinctions between TTS and PTS, we subjected 8-week-old C57BL/6N mice to noise-induced TTS (105 dB SPL for 60 min) or PTS (110 dB SPL for 120 min). Subsequently, we harvested their cochlea at 2 hours, 1 day, and 2 weeks after noise exposure, followed by conducting bulk RNA-sequencing (Figure 1). Before and after exposure to noise, the auditory brainstem response (ABR) and distortion product otoacoustic emission (DPOAE) were measured. After exposure to TTS-inducing noise, the hearing threshold at 30, 24, and 18 kHz increased abruptly to 80 dB SPL but returned to the original hearing threshold after 2 weeks (Figure 2A). In contrast, in the PTS group, hearing at high frequencies was impaired after 2 hours and 1 day, and did not recover to the original hearing threshold even after 2 weeks (Figure 2B). The shift in hearing thresholds observed in both TTS and PTS was evident in the response to click sounds (Figure 3A and 3B) and the amplitude of ABR wave 1 (Figure 3C and 3D). Additionally, we assessed the OHCs and IHCs in each cochlear tonotopic region 1 day and 2 weeks after exposure to TTS- and PTS-inducing noise (Figure 4). The observed loss of some OHCs showed no significant difference between the TTS and PTS groups. We conducted temporal transcriptomic analyses on mouse models of TTS and PTS, examining time points at 2 hours, 1 day, and 2 weeks after noise exposure. The gene expression of each sample was adjusted through normalization using the quantile method in  $\log_2$  (Transcripts Per Kilobase Million (TPM) + 1) units (Figure 5A). The correlation matrix showed that samples belonging to the same group exhibited comparable gene expression patterns (Figure 5B).

Principal component analysis (PCA) showed that datasets of TTS- and PTS-inducing noise stimulus were similar up to 1 day after noise exposure. However, after 2 weeks, the clusters of mice exposed to PTS-inducing noise were closer to the control (no exposure) dataset than to the clusters of mice exposed to TTS-inducing noise (Figure 6). Principal component analysis (PCA) revealed that the datasets generated by TTS- and PTS-inducing noise stimuli exhibited similarities up to 1 day following noise exposure. However, at the 2-week, the clusters representing mice exposed to PTS-inducing noise were more closely aligned with the control dataset (no exposure) than with the

clusters representing mice exposed to TTS-inducing noise (Figure 6). In the analysis of differentially expressed genes (DEGs), a total of 468 genes were identified, showing upregulation or downregulation in response to TTS- and PTS-induced noise exposure, respectively, compared to the control (no exposure). Over the course of time following noise exposure, genes associated with differentially expressed genes (DEGs) were primarily grouped into five clusters (Figure 7). Cluster 1 represented 38.5% of DEGs with elevated expression patterns one day after TTS- and PTS-inducing noise stimulation. Cluster 2 and Cluster 3 accounted for 4.2% and 12.6% of all DEGs, respectively, exhibiting expression patterns that increased immediately following TTS- and PTS-inducing noise stimulation. Cluster 3 exhibited an increased expression pattern from 2 hours to 1 day, while Cluster 2 showed an increased expression pattern only 2 hours after noise exposure. Cluster 4 (17%) showed an elevated level of expression 2 weeks after noise exposure in mice exposed to TTS, unlike PTS samples. Cluster 5 (27.7%) had no discernible expression pattern. The gene ontology (GO) analysis of DEGs using g:Profiler revealed a predominance of biological processes related to external stimuli, immune, and defense responses (Figure 8). Analysis of molecular function and cellular components also indicated a substantial number of DEGs linked to chemokine activity, signaling receptor regulator activity, and protein binding, distributed in extracellular regions and cytoplasm. Clusters 1, 2, and 3 exhibited similar transcriptional expression patterns after exposure to TTS and PTS-induced noise, with enriched Gene Ontology terms including responses to mechanical stimuli, ROS generation, response to hypoxia<sup>30</sup>, ERK signaling pathways<sup>31</sup>, ER stress<sup>32</sup>, and Toll-like receptor signaling pathways.<sup>33</sup> These pathways were previously identified to be activated by PTS-inducing noise exposure (Figure 9A). In contrast, Clusters 4 and 5 showed differences in transcriptional expression patterns between TTS and PTS-induced noise exposure samples, with an abundance of genes associated with tissue development, protein homooligomerization and endothelial cell differentiation (Figure 9B). In brief, transcriptome analysis over time following noise exposure revealed similarities but distinguishable changes in cochlear gene expression induced by both TTS and PTS-inducing noise.

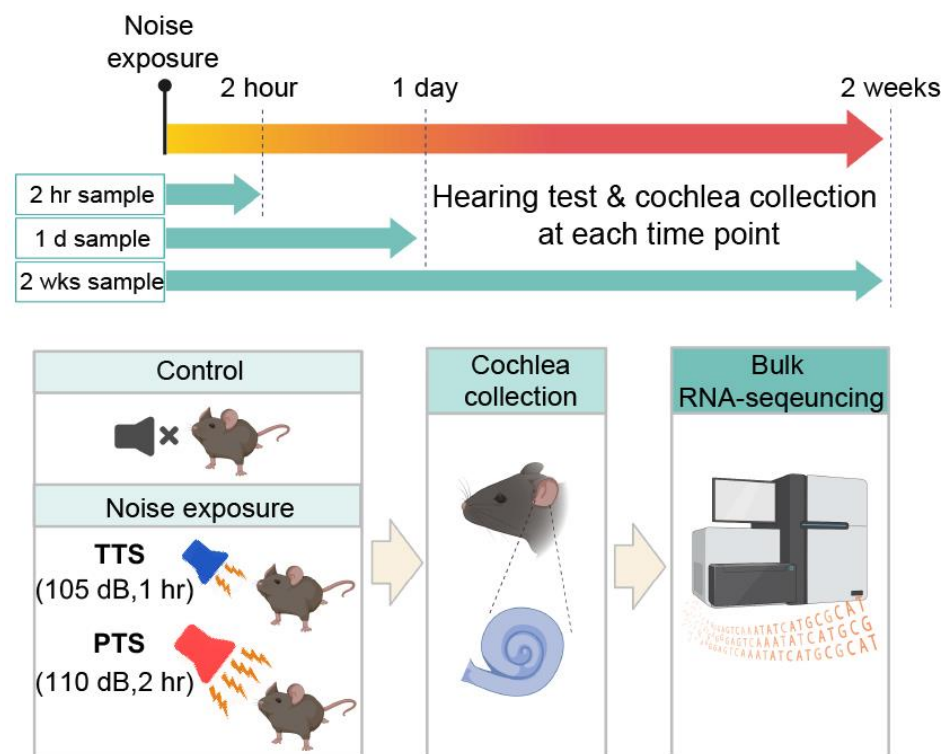


**Figure 1. Schematic representation of the experimental design.** Cochleae were collected from adult C57BL/6N mice at 2 hours, 1 day, and 2 weeks after exposure to TTS and PTS-induced noise, followed by RNA sequencing.

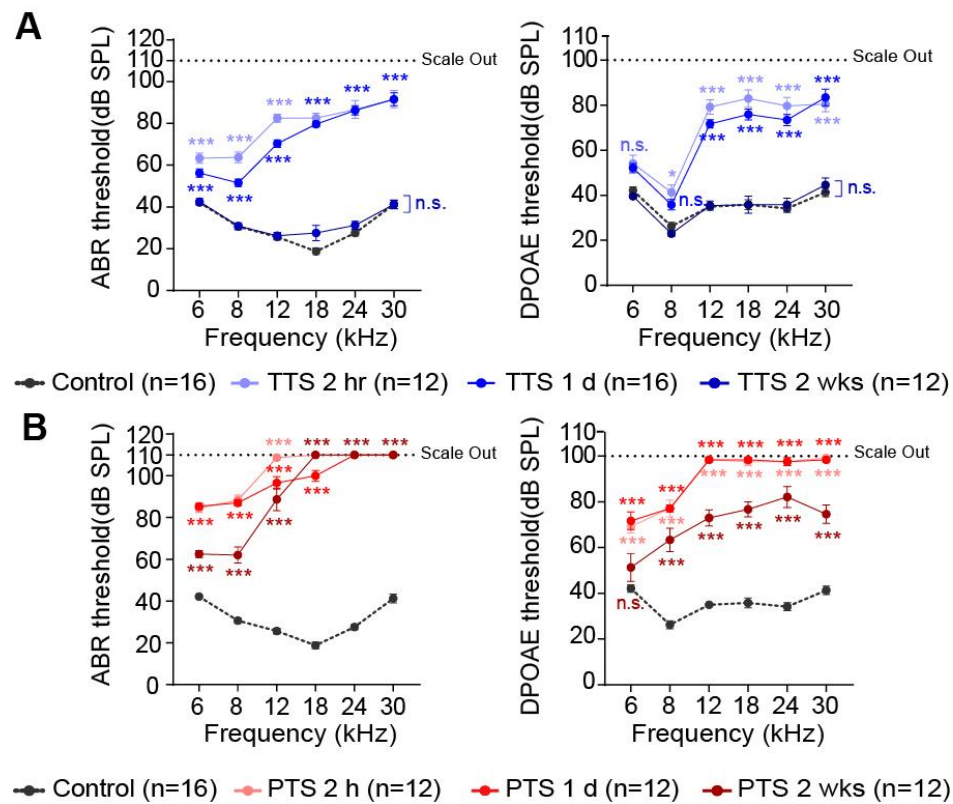


**Figure 2. Exposure to TTS-inducing noise results in hearing recovery after 2 weeks, whereas exposure to PTS-inducing noise leads to permanent hearing loss.** ABR and DPOAE thresholds in adult C57BL/6 mice after exposure to TTS (1 hour at 105dB SPL) and PTS (2 hours at 110dB SPL). (A) The thresholds increased by 1 day due to TTS-induced noise exposure returned to the original hearing levels by 2 weeks. (B) PTS-induced noise exposure showed significantly increased thresholds compared to TTS-induced noise exposure up to 1 day, and these thresholds did not recover even after 2 weeks, persistently increasing. The control group was not exposed to noise. Values and error bars are means  $\pm$  S.E.M. \*P < 0.05, \*\*P < 0.01, \*\*\*P < 0.001, n.s. not significant, two-way ANOVA with Bonferroni's post hoc analysis.

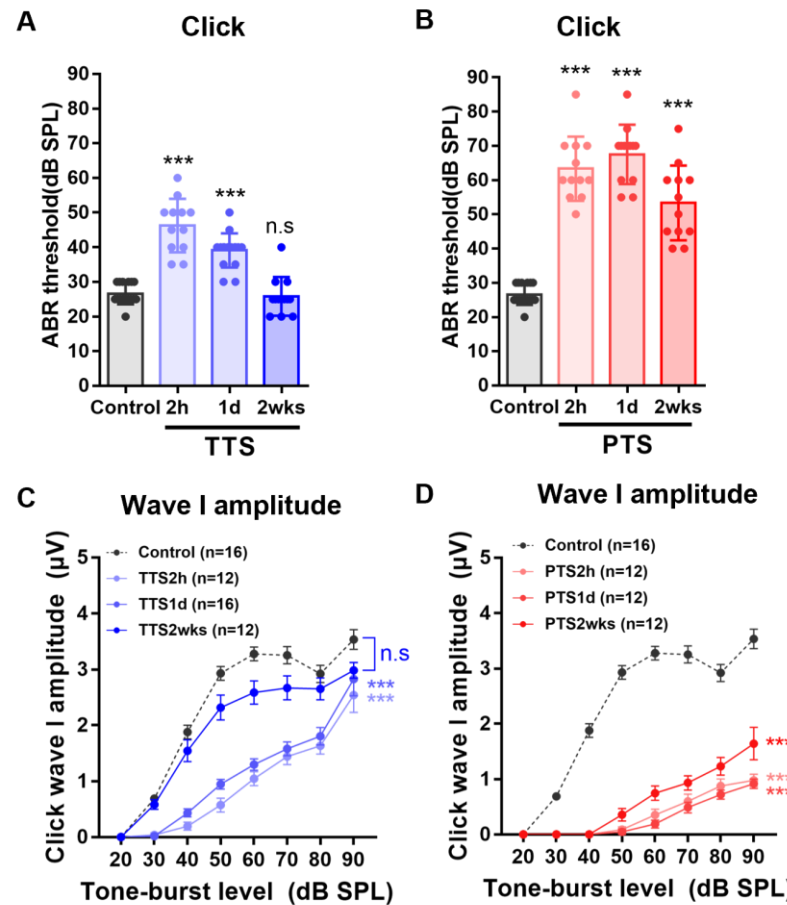


**Figure 3. Exposure to PTS-inducing noise impedes the recovery of click and wave I amplitudes.**

(A-B) ABR thresholds for a click stimulus in adult C57BL/6N mice exposed to TTS and PTS 2 hours, 1 day, and 2 weeks after noise exposure. The control group was not exposed to noise. (C-D) ABR wave I amplitude I/O function at each time course after TTS and PTS noise exposure. Values and error bars reflect means  $\pm$  S.E.M. Statistical comparisons were determined using two-way ANOVA with Bonferroni post hoc analysis (\*P < 0.05, \*\*P < 0.01, \*\*\*P < 0.001, n.s. non-significant).

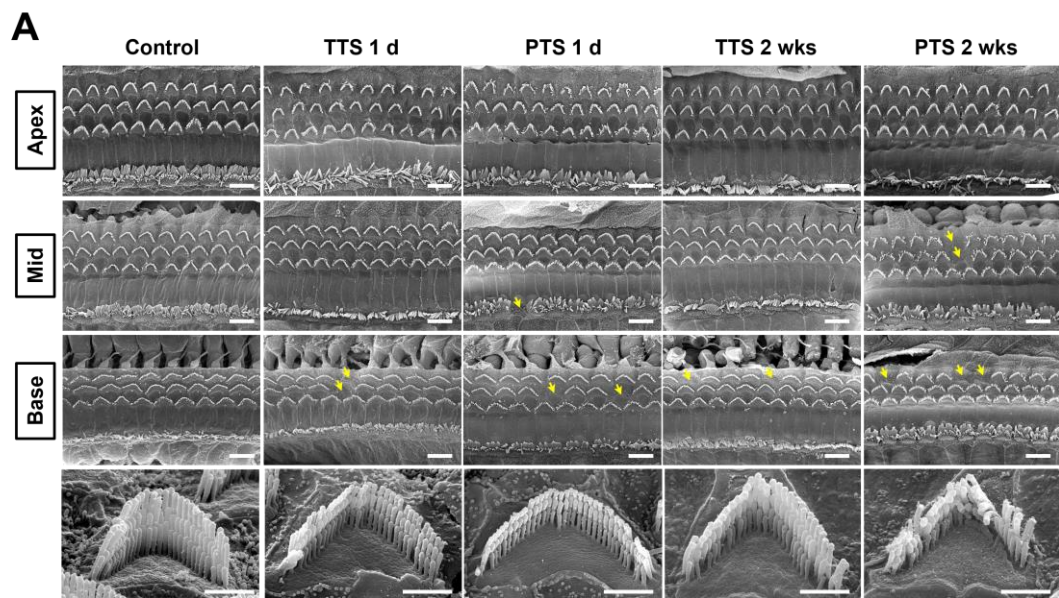


**Figure 4. Scanning Electron Microscope (SEM) images of the adult mouse cochlea after TTS and PTS-inducing noise exposure up to 2 weeks. (A)** Representative SEM images of apex, mid, and base region of cochlea 1 day and 2 weeks after exposure to TTS- and PTS-inducing noise. The yellow arrow indicates the damaged hair cell. Scale bars, 10  $\mu$ m.

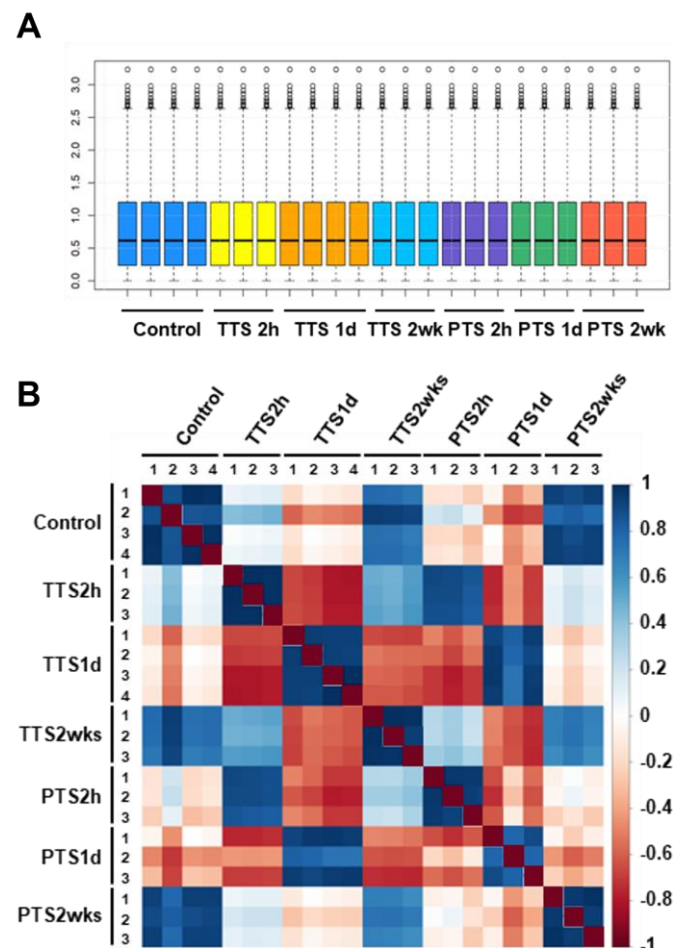


**Figure 5. Box plot and correlation matrix for RNA-sequencing in the cochlea after noise exposure.** (A) Box plot comparing the sample distribution levels of gene expression data following quantile normalization. (B) Spearman correlation matrices for all samples applying ANOVA with  $p<0.05$  criteria.

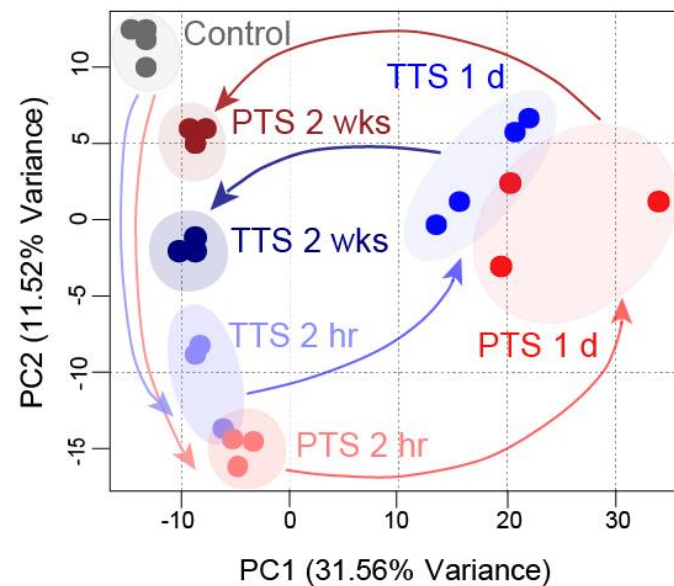


**Figure 6. Principal Component Analysis (PCA) plots of cochlear transcriptome data over time following TTS and PTS-induced noise exposure.** The gene expression patterns between TTS and PTS induction noise exposure were similar at 2 hours and 1 day after exposure. However, 2 weeks later, the group exhibiting gene expression patterns similar to the control group, which was not exposed to noise, was identified as the PTS group.

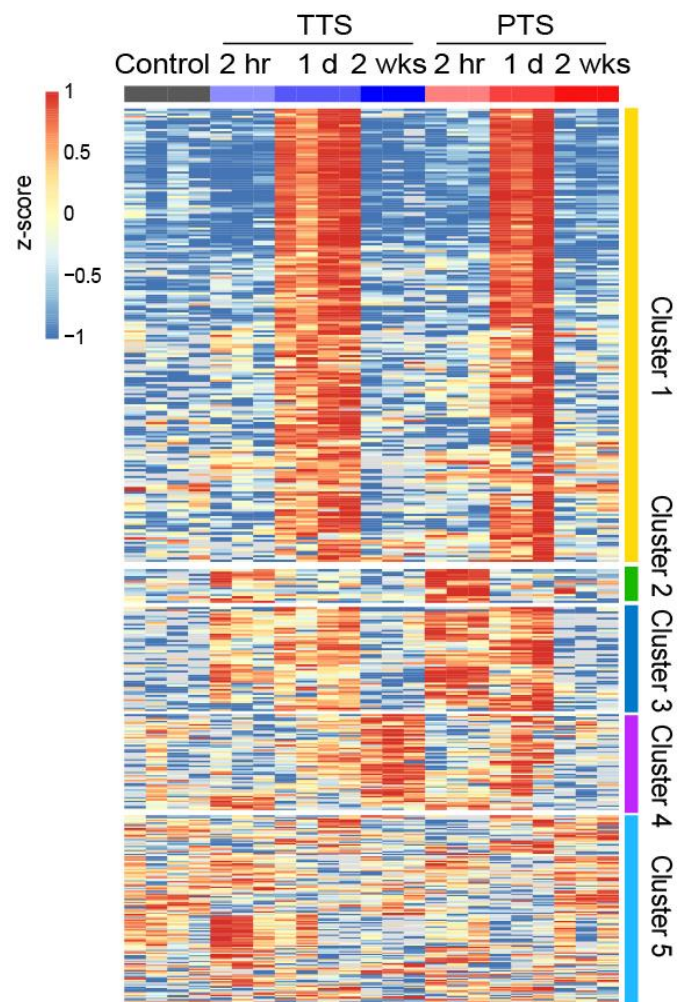


**Figure 7. Heatmap of Differentially Expressed Genes (DEGs) in samples exposed to TTS and PTS-induced noise exposure.** Hierarchical clustering of DEGs. The heatmap with  $\log_2(\text{TPM})$  values was normalized using z-score transformation. The expression of DEGs after TTS and PTS-induced noise exposure was categorized into 5 clusters.

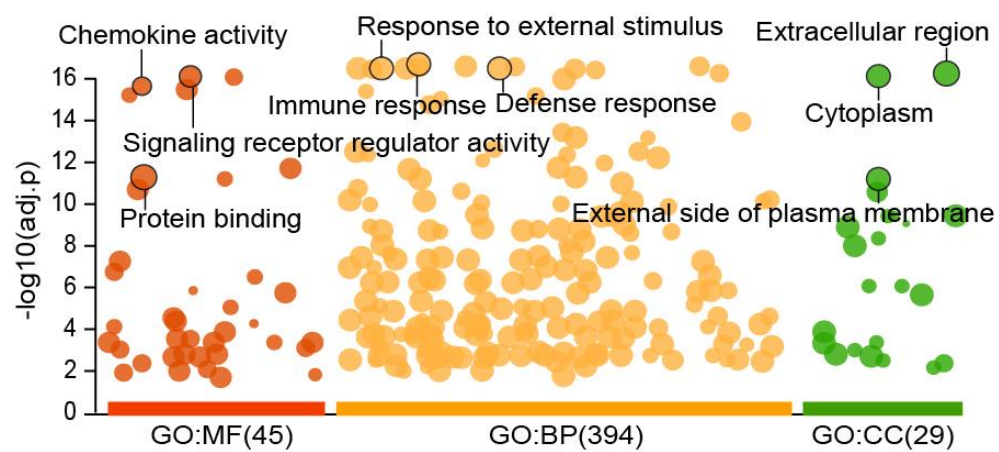


**Figure 8. Manhattan plot of Gene Ontology (GO) enrichment analysis results for all clusters of Differentially Expressed Genes (DEGs).** Each represents Molecular Function (MF), Biological Process (BP), and Cellular Component (CC) and the number of corresponding terms. The x-axis represents the GO terms, and the y-axis represents the negative decimal logarithm of the increased p-values. All enriched terms are marked on the graph with dots, and highlighted dots represent higher-level terms.

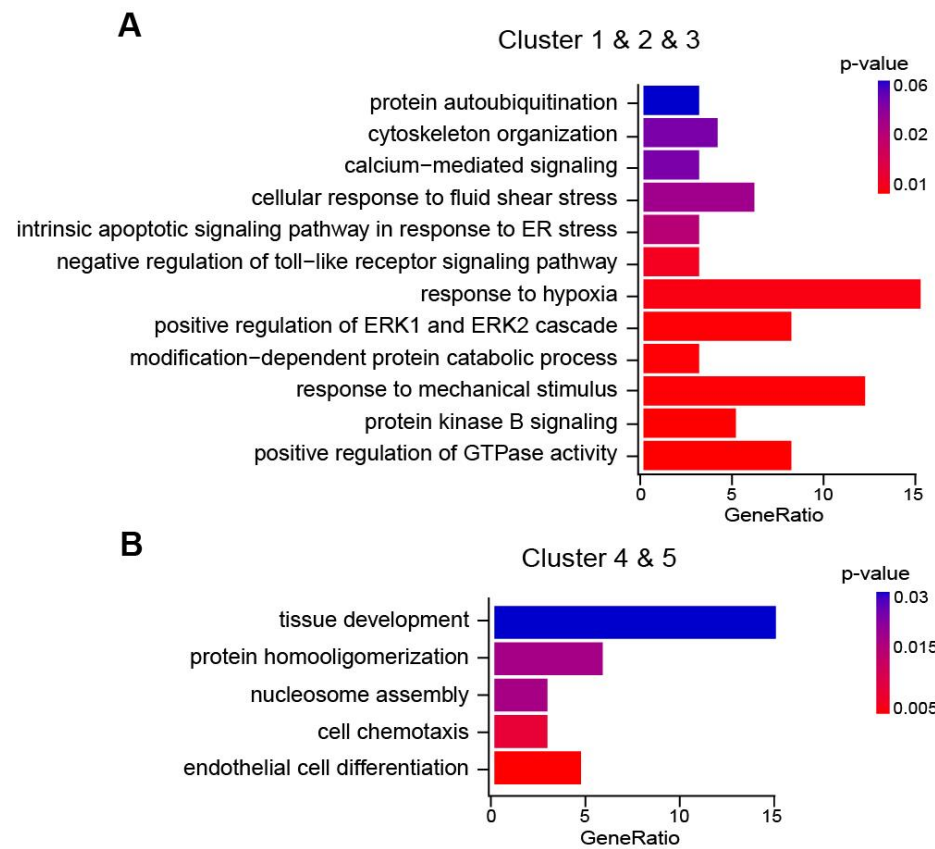


**Figure 9. Bar charts for the Gene Ontology (GO) analysis of DEGs.** (A) Biological process analysis results for Clusters 1, 2, and 3, which show similar gene expression patterns over time following TTS and PTS-inducing noise exposure, and (B) Clusters 4 and 5, which exhibit different expression patterns between TTS and PTS. The x-axis represents the proportion of total DEGs, and the color of the bars represents the p-values.

### 3.2 Noise exposure inducing TTS and PTS triggers ER stress and unfolded protein response

By utilizing Reactome and Enrichr, we performed pathway analysis of DEGs and discovered that these could be categorized into four distinct groups (Figure 10A).

The majority of DEGs were associated with immune response (32.6%), primarily related to B cell activation and cytokine signaling (Figure 10B).

Next, we investigated ER stress (31.7%) and Apoptosis (13.9%) pathways (Figure 10A). ER stress showed enrichment of terms involved in the response to misfolded proteins and the unfolded protein response (UPR) (Figure 10C). Terms categorized under apoptosis were associated with neuron death and cell death (Figure 10D). Interestingly, apoptosis enriched due to the ER stress response was revealed. Additionally, we quantified immune cell types through immune deconvolution analysis (Figure 11). Most immune cell types were monocytes, but no significant changes were observed due to noise exposure induced by TTS and PTS. Due to the cochlea's mosaic cell composition, a substantial portion of the cells remains unidentified.

Based on the RNA-sequencing results, the heatmap shows an increase in the expression of ER stress-related genes 1 day after noise exposure induced by TTS and PTS (Figure 12A). Additionally, gene set enrichment analysis (GSEA) verified the upregulation of genes related to the unfolded protein response (UPR) 1 day after exposure to noise inducing TTS and PTS (Figure 12B). The UPR is activated in response to a disturbance in protein homeostasis, initiated by the production of incorrectly folded proteins that fail to be properly degraded and accumulate within ER. To further confirm the induction of ER stress in the cochlea due to noise exposure induced by TTS and PTS, we conducted western blot analysis of cochlear lysates 3 days after each noise exposure. As a result, we observed increased protein levels of the chaperones, protein disulfide isomerase (PDI), and GRP78/BiP in the noise-exposed groups compared to the control group that was not exposed to noise (Figure 12C and 12D). Additionally, we used single-cell RNA sequencing (scRNA-seq) data from gEAR to identify cell types showing noise-induced transcriptional changes. Analyzing scRNA-seq datasets collected 1 day after exposure to noise inducing PTS<sup>28</sup>, we observed upregulation of ER stress and UPR-related genes in the sensory epithelia and some type 1A spiral ganglion neurons (Figure 13A and 13B). An aggresome is formed when there is an accumulation of misfolded and unfolded proteins within ER.<sup>34</sup> Previous studies have indicated that aggresomes accumulate in the apical regions of cochlear hair cells.<sup>35</sup> Three days after exposure to TTS- and



PTS-inducing noise, increased aggresome formation was observed (Figure 14A), and quantitative analysis revealed a significant accumulation compared to the control group in both OHCs (Figure 14B) and IHCs (Figure 14C).

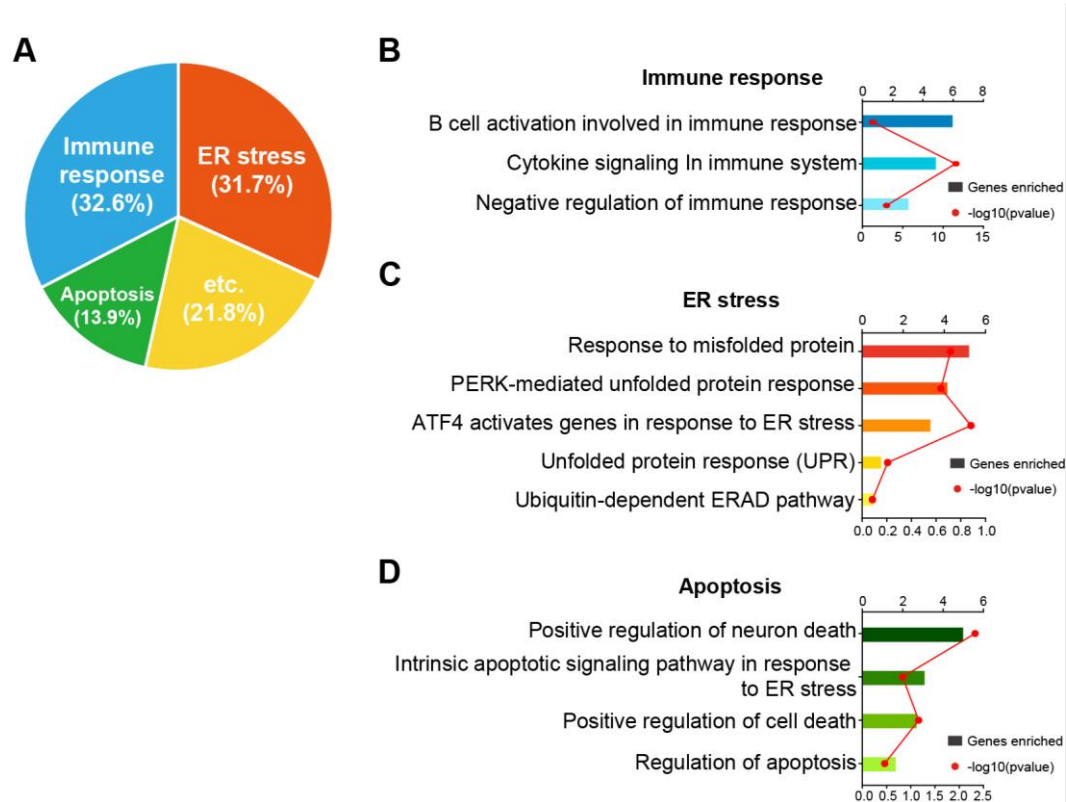


**Figure 10. Pie charts and bar charts representing the Reactome and Enrichr pathway analysis of DEGs.** (A) Each section of the circular chart represents the proportion of genes attributed to specific pathways. They are categorized into a total of 4 pathways. (B-D) Show enhanced Gene Ontology terms for immune response (C), endoplasmic reticulum (ER) stress (B), and apoptosis (D). The bars represent the gene enrichment ratio for each term, and the red lines indicate  $-\log_{10}(p\text{value})$ .

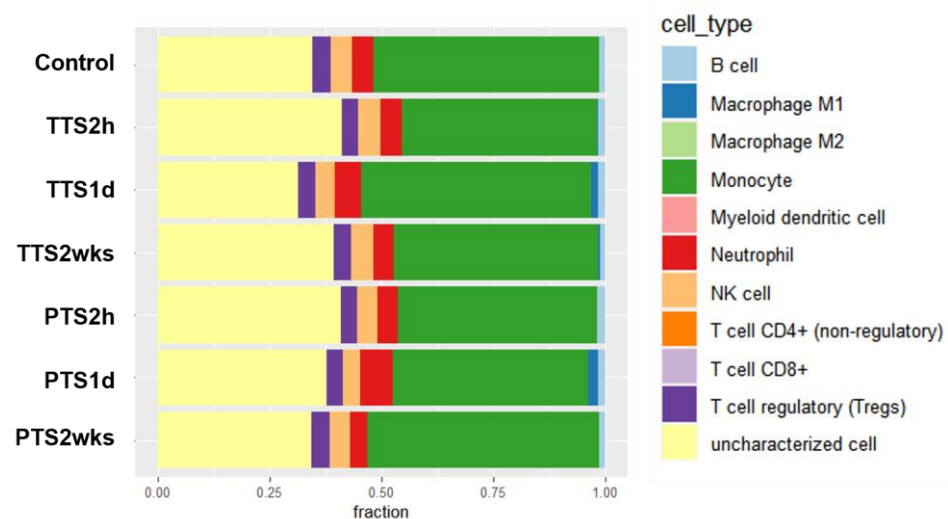


**Figure 11. Immune cell deconvolution analysis based on RNA sequencing.** The proportion of immune cells up to 2 weeks after TTS and PTS-induced noise exposure did not show any significant difference. The x-axis represents the proportion of each cell type, while the y-axis represents each sample.

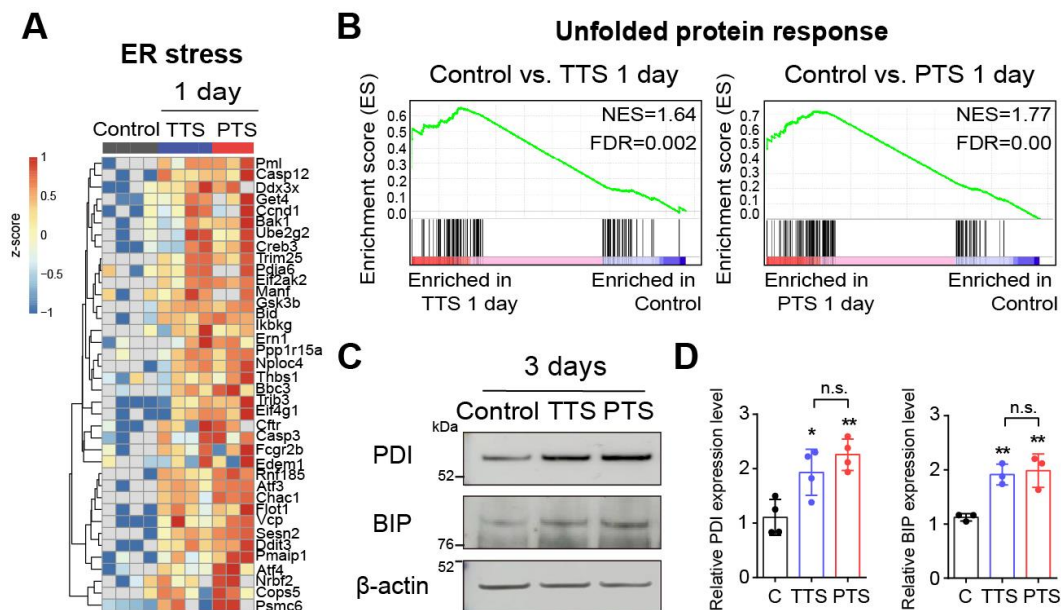


**Figure 12. Exposure to TTS and PTS-induced noise triggers ER stress and UPR in the cochlea.**

(A) A heatmap depicting the expression of endoplasmic reticulum (ER) stress-related genes in the cochlea exposed to TTS and PTS noise induction 1 day after exposure, based on RNA sequencing data. Gene expression was normalized using z-score transformation on  $\log_2(\text{TPM})$  values. (B) Gene set enrichment analysis of unfolded protein response (UPR) pathways one day after exposure to TTS (left) and PTS (right) noise induction, compared to unexposed control group. NES represents normalized enrichment score. (C) Representative Western blot images showing the expression of PDI, BiP, and  $\beta$ -actin in cochlea lysates collected three days after TTS and PTS noise exposure. (D) Quantification of PDI (left) and BiP (right) western blot results.

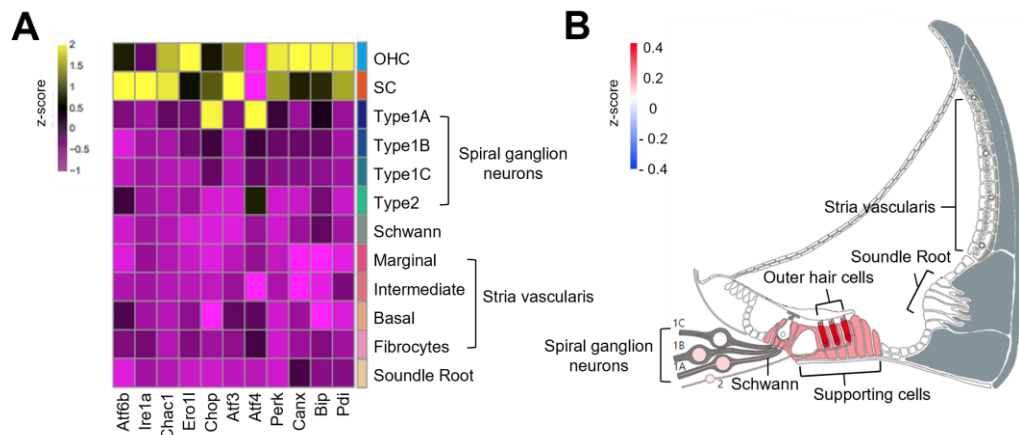


**Figure 13. Expression of ER stress and UPR-related factors in each cell type of cochlea 1 day after exposure to PTS-inducing noise.** (A) Heatmap of unfolded protein response (UPR) marker gene sets for each cell type 1 day after PTS-induced noise exposure. The gEAR database for scRNA sequencing data of the cochlea was applied. Normalization was performed using z-score transformation on  $\log_2(\text{TPM})$  values. (B) Schematic diagram showing the cell-type-specific gene expression related to unfolded protein response one day after PTS noise exposure.

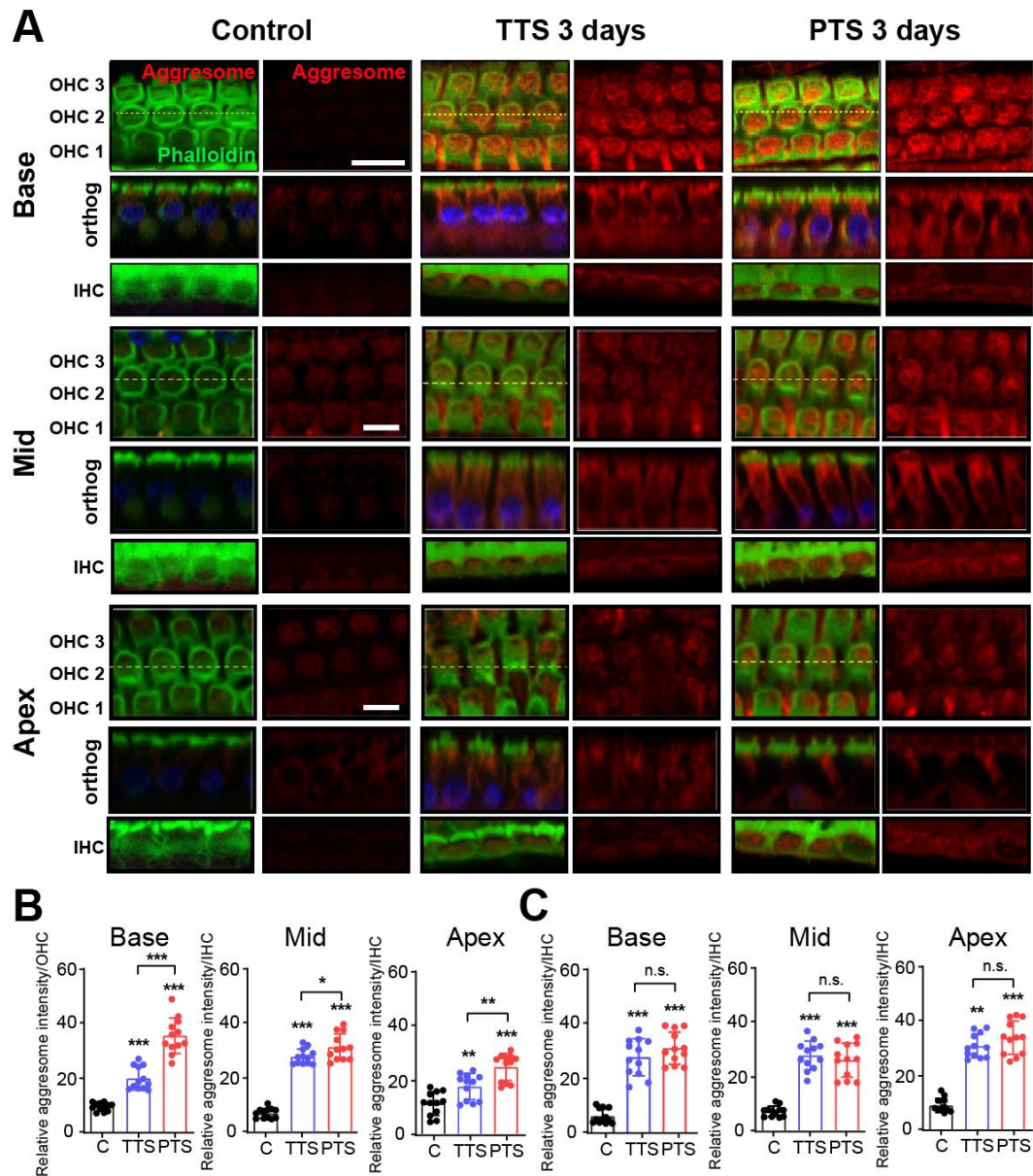


**Figure 14. Exposure to TTS and PTS-induced noise induces aggresome formation in cochlear.**

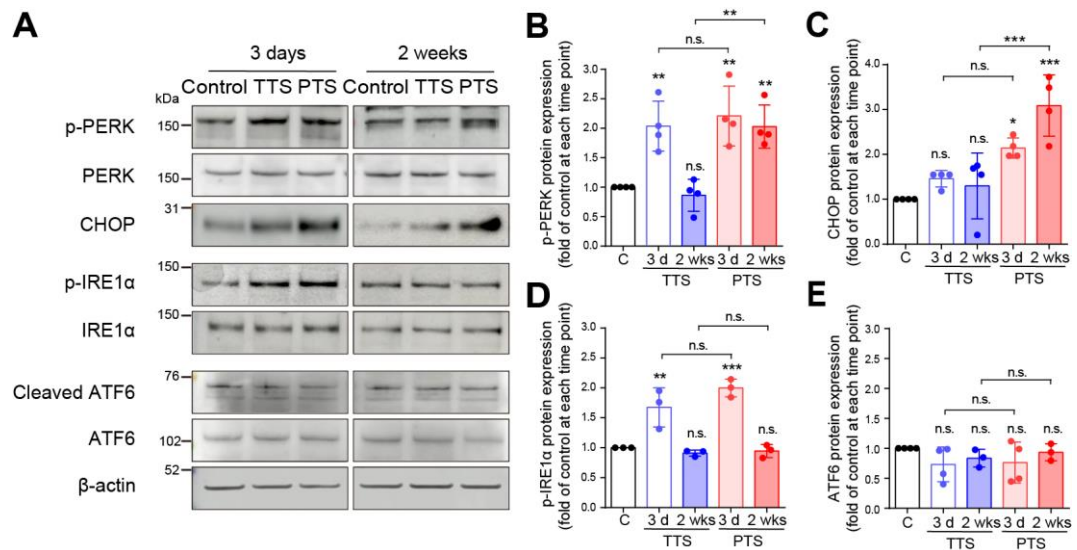
(A) After 3 days of TTS and PTS noise exposure, aggresome staining was performed in the base, mid, and apex regions of the cochlea. The control group was not exposed to noise. (B) Quantitative analysis of aggresomes in outer hair cells (OHCs) and (C) inner hair cells (IHCs). The yellow horizontal line indicates the position of orthogonal sections. Scale bar, 10 $\mu$ m. Data are represented as mean  $\pm$  SEM. \*P < 0.05, \*\*P < 0.01, one-way ANOVA with Bonferroni post hoc test.

### **3.3 The protein kinase R-like endoplasmic reticulum kinase (PERK) branch of UPR is continuously activated in response to PTS-inducing noise**

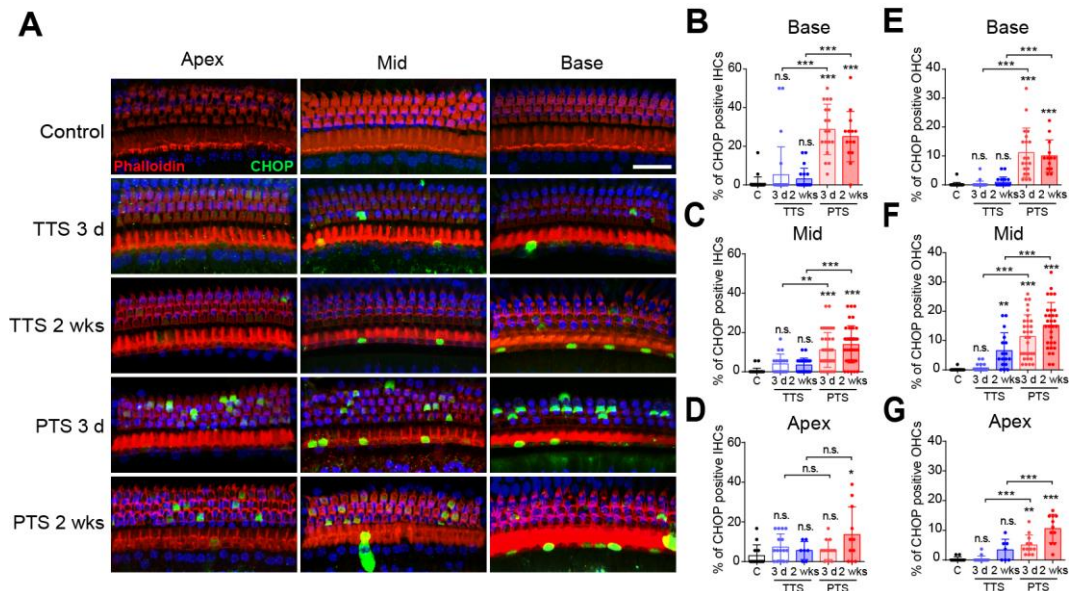
The Unfolded Protein Response (UPR) comprises three branches: PERK, IRE1 $\alpha$ , and ATF6. BiP binds to these receptors, and upon detecting unfolded or misfolded proteins, the receptors dissociate from the chaperones, triggering downstream signaling through the mediator. These pathways simultaneously regulate transcription, temporarily reduce protein import into the ER, and activate apoptosis if ER stress persists without resolution. To investigate the branches activated by TTS- and PTS-inducing noise exposure, the protein levels of the three receptors were examined 3 days and 2 weeks after noise exposure (Figure 15A).<sup>36-38</sup> Remarkably, there were distinctions in the activation of the PERK pathway between TTS- and PTS-inducing noise. By the 2-week mark, corresponding to the period of hearing recovery, the increased expression of phosphorylated PERK (p-PERK) induced by 3 days of exposure to TTS-inducing noise returned to its baseline level. Conversely, the level of p-PERK, elevated by exposure to PTS-inducing noise, remained elevated for 2 weeks (Figure 15B). In contrast to IRE1 $\alpha$  and ATF6, which mainly work towards alleviating ER stress, the PERK branch inhibits protein translation, thus concurrently mitigating ER stress and triggering CHOP, a pro-apoptotic factor. Furthermore, we noticed differences in CHOP expression between TTS- and PTS-inducing noise. Unlike p-PERK, which reverted to baseline expression levels 2 weeks after exposure to TTS-inducing noise, CHOP expression was not induced by TTS.

The CHOP expression exhibited a significant increase from 3 days to 2 weeks after exposure to PTS-inducing noise (Figure 15C). p-IRE1 $\alpha$  showed elevation due to noise exposure compared to the control and returned to the baseline level after 2 weeks in both TTS and PTS (Figure 15D), while ATF6 remained unaffected by noise in both TTS and PTS (Figure 15E). Next, we investigated the time course of CHOP expression in the cochlea following TTS- and PTS-inducing noise exposure (Figure 16A). The gEAR database indicated a substantial rise in ER stress-related factors in cochlear hair cells following exposure to PTS-inducing noise (Figure 13). The CHOP expression was detected in IHCs and OHCs following exposure to TTS- and PTS-inducing noise (Figure 16A). Quantitative analysis revealed that CHOP staining was exclusively present in the central cochlear OHCs two weeks after noise exposure in the TTS group (Figure 16E-16G). Conversely, in the PTS group, CHOP expression remained consistently elevated from 3 days to 2 weeks in both IHCs and OHCs

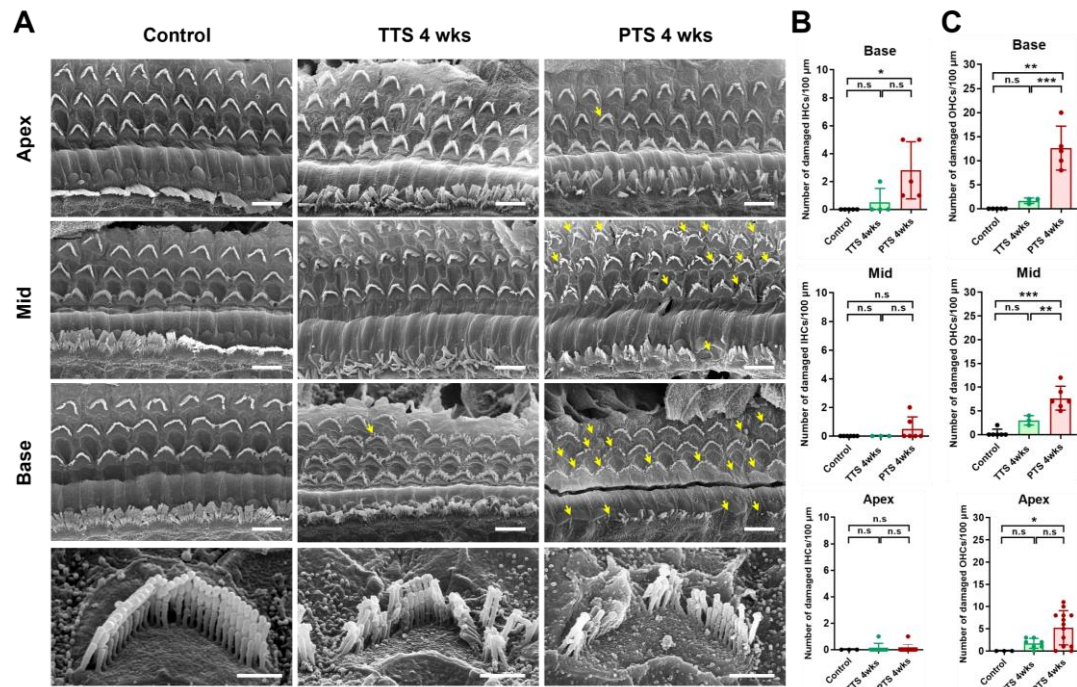
across all cochlear regions, except for the apical IHCs after 3 days of noise exposure. Two weeks following noise exposure in TTS group, quantitative analysis showed that CHOP staining was only seen in the middle cochlear OHCs. In contrast, following 3 days of noise exposure, CHOP expression in both IHCs and OHCs in every cochlear region—apart from the apical IHCs—remained persistently higher in PTS group (Figure 16B–16G). Prior research has shown that during 2 weeks of noise exposure, there is no discernible change in the morphology of hair cells between TTS and PTS (Figure 4). We investigated into whether the structure of hair cells was affected by the increased expression of CHOP driven on by PTS-inducing noise (Figure 17A). Samples exposed to PTS-inducing noise showed a significant rise in abnormal IHCs (Figure 17B) and OHCs (Figure 17C) after 4 weeks of noise exposure. To summarize, noise that induces TTS and PTS increased the expression of p-PERK and p-IRE1 $\alpha$  in the cochlea. The PERK pathway is regulated differently in TTS and PTS. In the TTS group, p-PERK and p-IRE1 $\alpha$  reverted to baseline levels after 2 weeks, when hearing was restored. Unlike the TTS group, in the PTS group, CHOP, a pro-apoptotic factor, was increased and p-PERK was continuously activated.



**Figure 15. The PERK branch remains continuously activated up to 2 weeks following PTS-induced noise exposure.** (A) Representative Western blot images of proteins associated with unfolded protein response branches in cochlea at 3 days and 2 weeks after noise exposure. (B-E) Quantification of lane intensities for phosphorylated PERK (B), CHOP (C), phosphorylated IRE1 $\alpha$  (D), and ATF6 (E). Each protein expression was normalized to  $\beta$ -actin and then to the unexposed control. Data are shown as mean  $\pm$  SEM, \* $P$   $<$  0.05, \*\* $P$   $<$  0.01, \*\*\* $P$   $<$  0.001, n.s. not significant, one-way ANOVA with Bonferroni's post-hoc test.



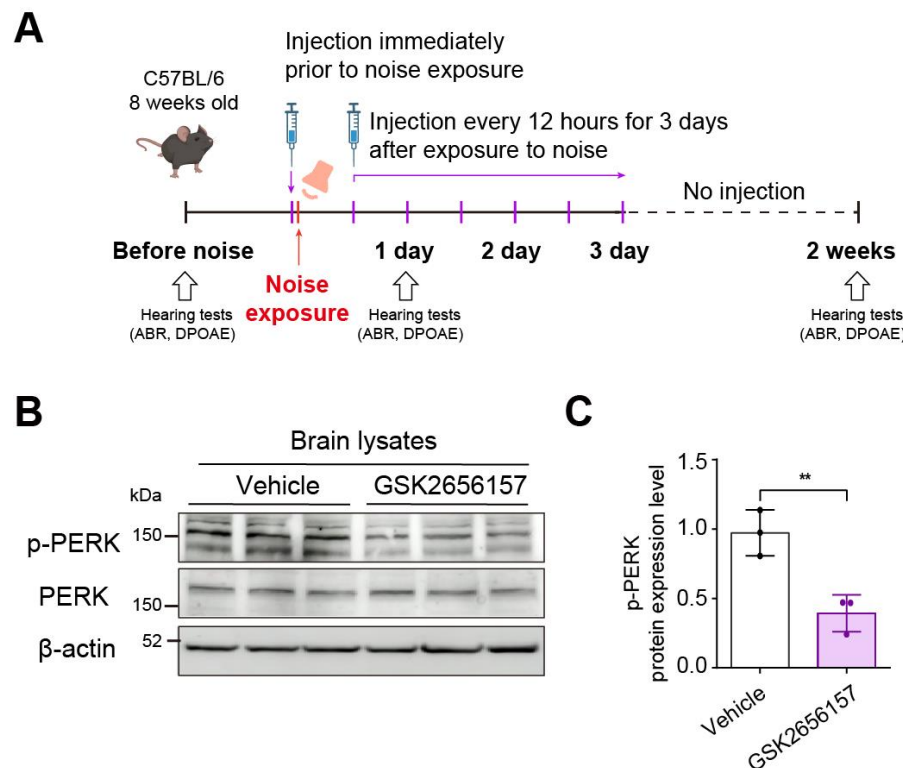
**Figure 16. PTS-induced noise exposure induces the expression of CHOP in the hair cells of the cochlea.** (A) Whole-mount immunostaining of the cochlea from control and noise-exposed mice with Phalloidin (red) and CHOP (green). Scale bars, 30  $\mu$ m. (A-G) Quantitative analysis of CHOP-stained inner (B-D) and outer (E-G) hair cells. The percentage of CHOP-positive cells in the 130  $\mu$ m region of the cochlea were counted and quantified as a percentage. Data are expressed as means  $\pm$  SEM. \*P < 0.05, \*\*P < 0.01, \*\*\*P < 0.001, n.s. not significant, one-way ANOVA with Bonferroni's post-hoc analysis.



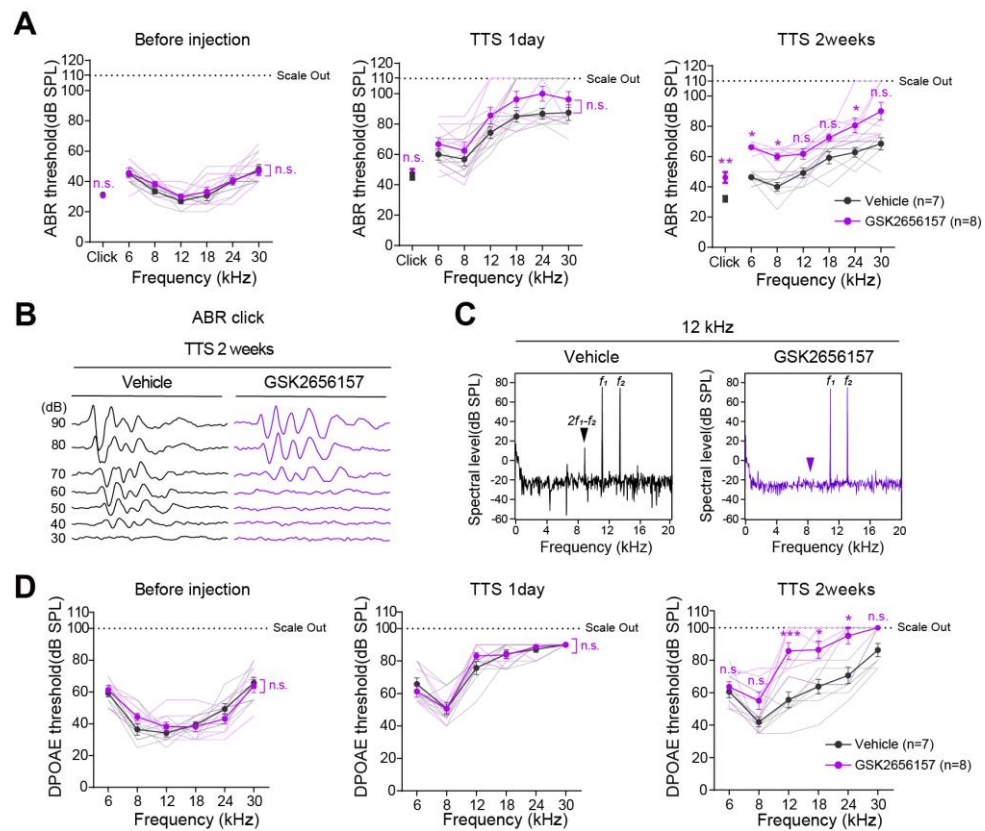
**Figure 17. Scanning Electron Microscope (SEM) images of adult mouse cochlea after 4 weeks of TTS- and PTS-inducing noise exposure.** (A) Representative SEM images of base, mid, apex region of cochlea 4 weeks after exposure to TTS- and PTS-inducing noise. The bottom images depict representative damaged outer hair cells (OHCs) in the base region. The yellow arrow indicates the damaged hair cell. Scale bars, 1  $\mu$ m. Scale bars, 10  $\mu$ m. (B-C) Quantitative analysis of damaged OHCs (B) and IHCs (C). The damaged hair cells in the 100  $\mu$ m region of the cochlea were counted and quantified. Values and error bars reflect means  $\pm$  S.E.M. Statistical comparisons were determined using two-way ANOVA with Bonferroni post hoc analysis (\*P < 0.05, \*\*P < 0.01, \*\*\*P < 0.001, n.s. non-significant).

### **3.4 Inhibition of PERK activity before and after TTS-inducing noise exposure interferes with hearing recovery**

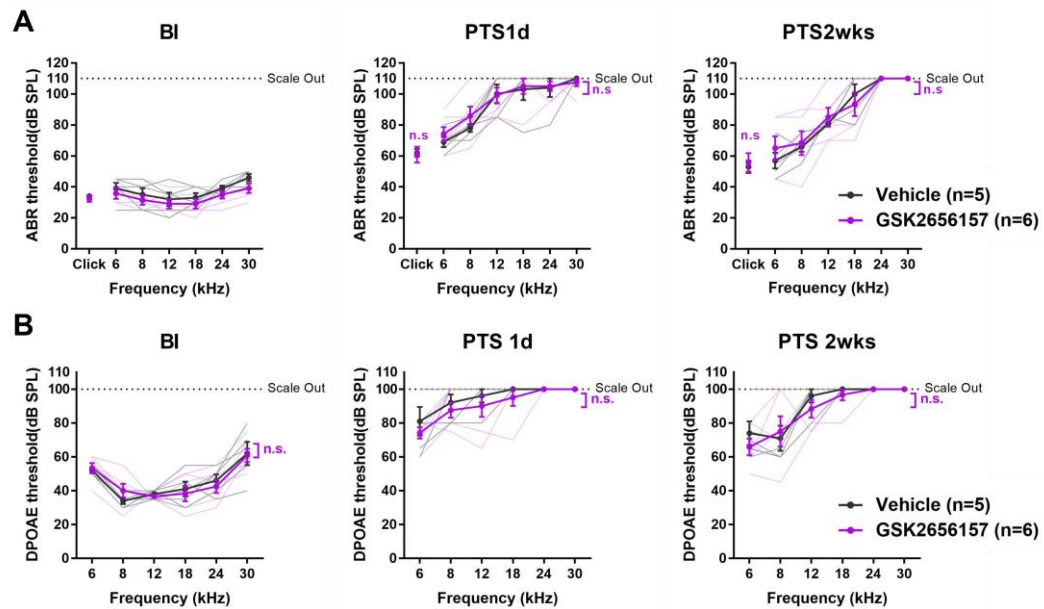
Next, we investigated whether noise-induced PERK activation was beneficial or deleterious to hearing recovery. Adult mice were administered intraperitoneal injections of GSK2656157 (40 mg/kg), a known p-PERK inhibitor, before noise exposure. Additionally, after the noise exposure, six more injections were administered at 12-hour intervals (Figure 18A). Next, following 3 days of exposure to TTS-inducing noise, we observed the expression of p-PERK in the brain lysates of the vehicle and GSK2656157 treatment groups (Figure 18B). Western blot showed that 40 mg/kg of GSK2656157 effectively inhibited PERK phosphorylation (Figure 18C). After 1 day of exposure to TTS-inducing noise, no difference in ABR thresholds was observed between mice treated with the vehicle and those treated with the p-PERK inhibitor. However, at the 2-week mark, the mice treated with the p-PERK inhibitor showed a significant increase in ABR thresholds at specific frequencies compared to mice treated with the vehicle, even though they were exposed to TTS-inducing noise (Figure 19A). In the observation of responses to ABR click sounds, it was shown that 2 weeks after exposure to TTS-inducing noise, mice treated with the vehicle exhibited a response of approximately 40 dB to the click sound stimulus, which recovered to the pre-noise exposure level. In contrast, mice treated with the p-PERK inhibitor showed an ABR threshold of 70 dB, indicating that hearing recovery did not occur (Figure 19B). The representative DPOAE amplitudes at 12 kHz for mice treated with vehicle and PERK inhibitor are shown in Figure 19C. The DPOAE thresholds showed no difference between the vehicle-treated mice and the p-PERK inhibitor-treated mice one day after, but after 2 weeks of noise exposure, mice treated with the p-PERK inhibitor exhibited significantly higher DPOAE thresholds at 24, 18, and 12 kHz compared to mice treated with the vehicle (Figure 19D). We also conducted the experiment under PTS-induced noise conditions. However, there were no significant differences observed in the groups administered with the vehicle and PERK inhibitor (Figure 20A and 20B). Taken together, these results imply that early PERK activation after noise exposure is required for hearing recovery.



**Figure 18. Treatment with the PERK inhibitor, GSK2656157 before and after exposure to TTS-inducing noise leads to a decrease in p-PERK expression.** (A) Schedule of intraperitoneal injection of the PERK inhibitor. Intraperitoneal injections were performed at 12-hour intervals from just before exposure to TTS-induced noise until 3 days after exposure. (B) Western blot image of p-PERK in brain lysate treated with the PERK inhibitor, GSK2656157. (C) Quantitative analysis of p-PERK in the GSK2656157-treated group compared to the vehicle-treated group. Each protein expression was normalized to  $\beta$ -actin and then to the unexposed control. Data are shown as mean  $\pm$  SEM, \*P < 0.05, \*\*P < 0.01, \*\*\*P < 0.001, n.s. not significant, one-way ANOVA with Bonferroni's post-hoc test.



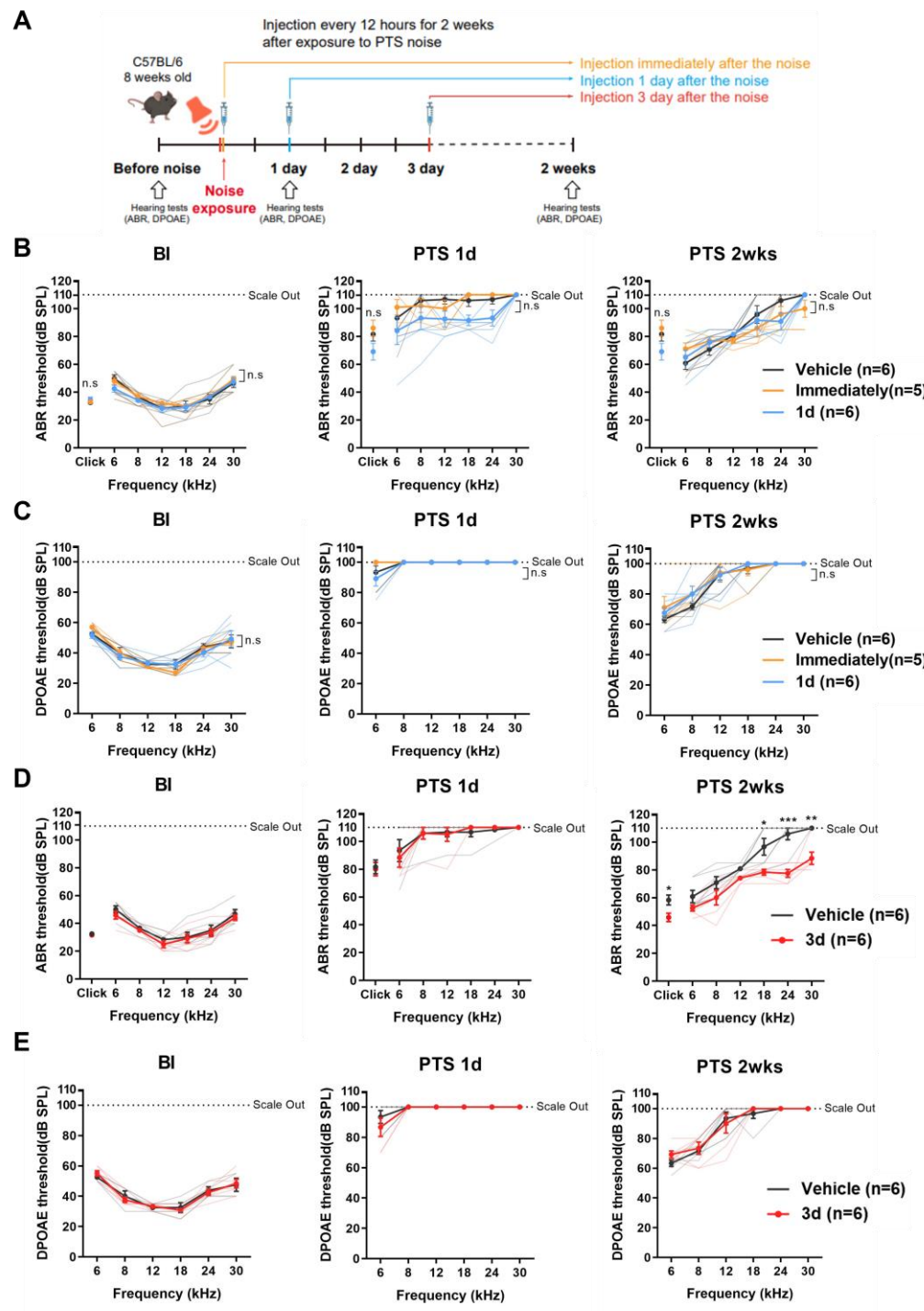
**Figure 19. Inhibition of PERK early after TTS-inducing noise exposure disrupts hearing recovery.** (A) Auditory Brainstem Response (ABR) thresholds in mice treated with vehicle (gray) or PERK inhibitor (purple) at 1 day and 2 weeks after TTS-inducing noise exposure. (B) Representative ABR waveforms including click stimuli recorded from mice treated with vehicle (gray) and PERK inhibitor (purple) 2 weeks after TTS-inducing noise exposure. (C) Representative 12 kHz spectra of Distortion Product Otoacoustic Emissions (DPOAE) recordings from mice treated with vehicle and PERK inhibitor. The spectral peaks of the two stimulus tones are indicated as  $f_1$  and  $f_2$ , and the measured DPOAE is represented as  $2f_1-f_2$ . (F) DPOAE threshold in mice treated with vehicle (gray) or PERK inhibitor (purple). Values and error bars represent mean  $\pm$  S.E.M. \*P < 0.05, \*\*P < 0.01, \*\*\*P < 0.001, n.s. Not significant by two-way ANOVA with Bonferroni post hoc analysis.



**Figure 20. The initial inhibition of PERK activity following PTS-inducing noise exposure does not affect in hearing recovery.** (A) ABR and (B) DPOAE threshold of mice treated with vehicle (gray) or PERK inhibitor (purple) 1 day and 2 weeks after PTS-inducing noise exposure. Values and error bars are means  $\pm$  S.E.M. \*P < 0.05, \*\*P < 0.01, \*\*\*P < 0.001, n.s. not significant, two-way ANOVA with Bonferroni post hoc analysis.

### 3.5 The inhibition of persistent activation of PERK mitigates noise-induced hearing loss

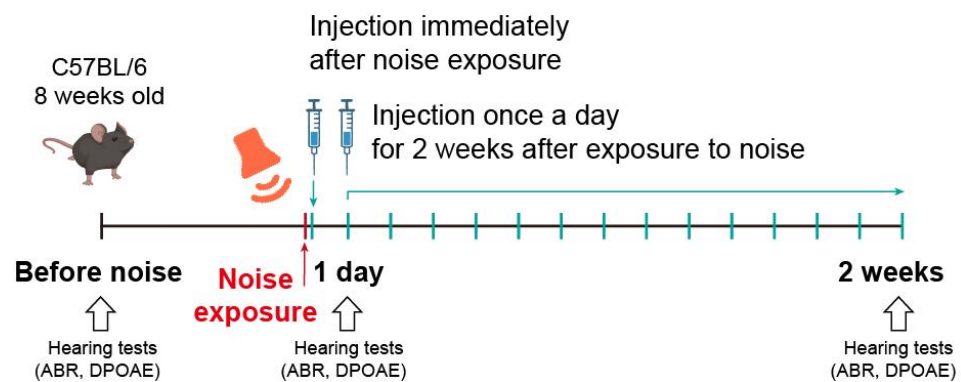
Based on the previous findings confirming the necessity of initial PERK activation in the hearing recovery process, we investigated the impact of inhibiting the persistent activation of PERK observed in PTS on hearing. To explore this, we began at each of three time points and intraperitoneally delivered the p-PERK inhibitor, GSK2656157, at 12-hour intervals: PTS-inducing noise exposure can occur 1) immediately, 2) 1 day later, and 3) 3 days later, up to 2 weeks later (Figure 21A). For the following 2 weeks after noise exposure, injection of the p-PERK inhibitor both immediately and 1 day after did not affect hearing loss due to PTS (Figure 21B and 21C). Surprisingly even though they were exposed to PTS-inducing noise, the group that received the p-PERK inhibitor three days after noise exposure exhibited a significant improvement in ABR thresholds at 30, 24, 18 kHz compared to the vehicle group (Figure 21D). The DPOAE threshold did not significantly differ between the control group and the group that was given treatment after 3 days (Figure 21E). In summary, the initial activation of PERK after noise exposure is a necessary step for hearing recovery. However, persistent activation of PERK up to 2 weeks after noise exposure hinders hearing recovery and administering a PERK inhibitor starting from 3 days after noise exposure suppresses PERK activity, contributing to hearing restoration.



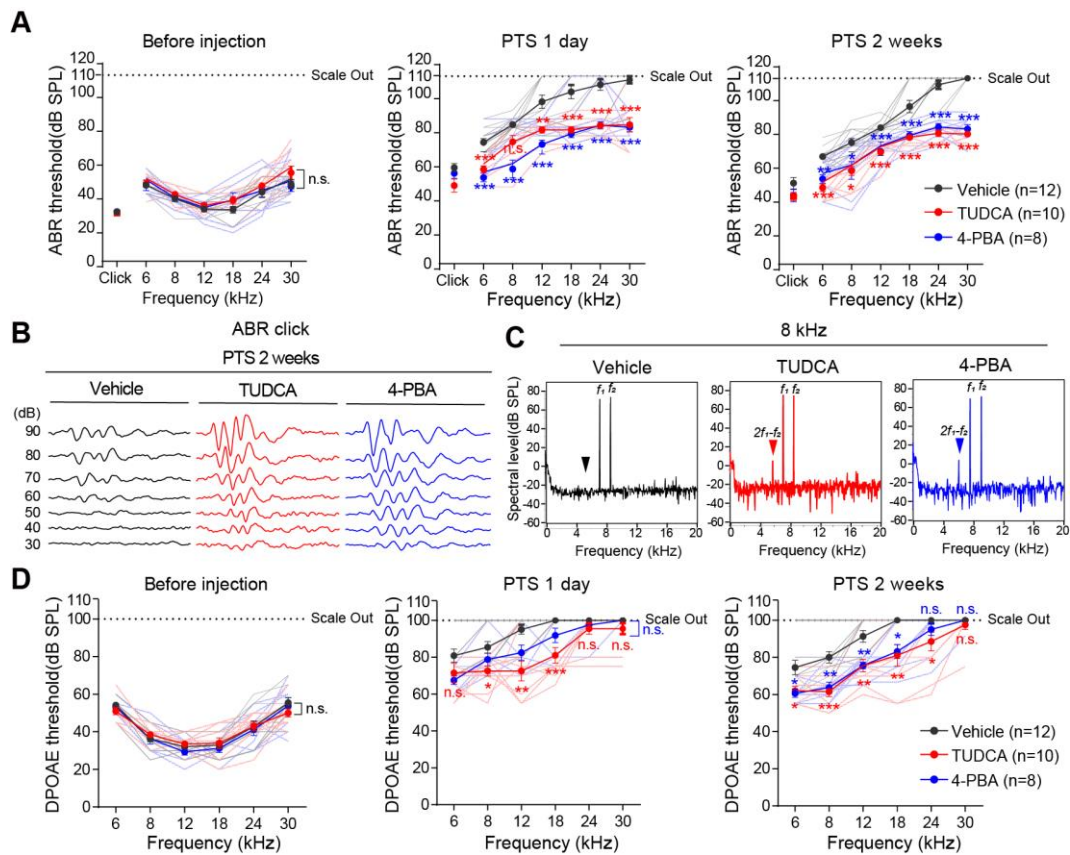
**Figure 21. Inhibition of sustained activation of PERK following PTS-inducing noise exposure is beneficial for hearing recovery.** (A) Schedule of intraperitoneal PERK inhibitor administration. (B) Auditory brainstem response (ABR) thresholds in mice treated with vehicle (gray) or PERK inhibitor immediately (yellow) and 1 day (blue) after PTS-induced noise exposure. (C) Distortion product otoacoustic emission (DPOAE) thresholds of mice treated with vehicle (gray) or PERK inhibitor immediately (yellow) and 1 day (blue) after PTS-induced noise exposure. (D) ABR threshold shifts of mice treated with vehicle (grey), 3 days (red) after PTS-induced noise exposure. (E) DPOAE thresholds of mice treated vehicle (gray) and the group treated 3 days after exposure to PTS-inducing noise (red). Values and error bars are means  $\pm$  S.E.M. \*P < 0.05, \*\*P < 0.01, \*\*\*P < 0.001, n.s. not significant, two-way ANOVA with Bonferroni's post-hoc analysis.

### **3.6. Administration of pharmacological chaperones immediately after noise exposure protects noise-induced hearing loss**

We evaluated whether reducing the initial ER stress occurring after noise exposure could prevent noise-induced hearing loss. We applied 4-phenylbutyric acid (4-PBA) and tauroursodeoxycholic acid (TUDCA), two chemical chaperones that are known to reduce ER stress. Adult mice exposed to PTS-inducing noise were given intraperitoneal injections of 300 mg/kg of each of the two chemical chaperones as soon as possible, and they were thereafter given injections every day for up to two weeks (Figure 22). Mice treated with TUDCA or 4-PBA had significantly lower ABR thresholds at almost all frequencies 1 day after PTS-inducing noise exposure than mice treated with vehicles. Two weeks after exposure to PTS-inducing noise, the reduced thresholds due to chemical chaperone treatment remained sustained (Figure 23A). Mice treated with the vehicle showed a response to click stimuli at approximately 60dB, while mice treated with TUDCA or 4-PBA exhibited click thresholds 30dB lower than those of vehicle-treated mice despite exposure to PTS-inducing noise (Figure 23B). The representative DPOAE amplitudes for the vehicle- and chemical chaperone-treated groups are shown at 8 kHz in Figure 23C. One day after exposure to PTS-inducing noise, the group treated with chemical chaperones showed a significant decrease in DPOAE thresholds compared to the vehicle-treated group. Despite exposure to PTS-inducing noise, the hearing threshold reduction in mice treated with pharmacological chaperones persisted for 2 weeks (Figure 23D).



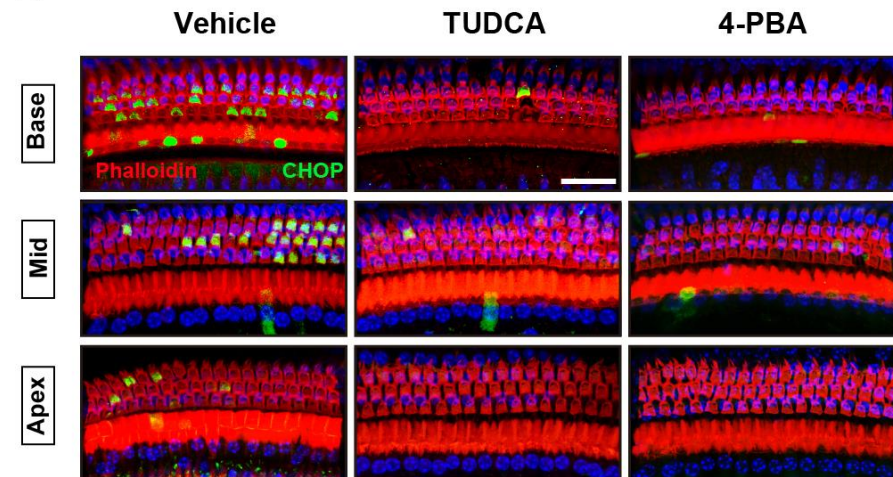
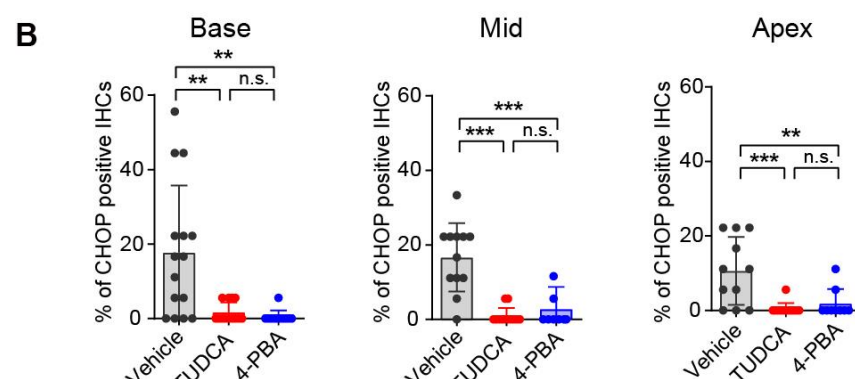
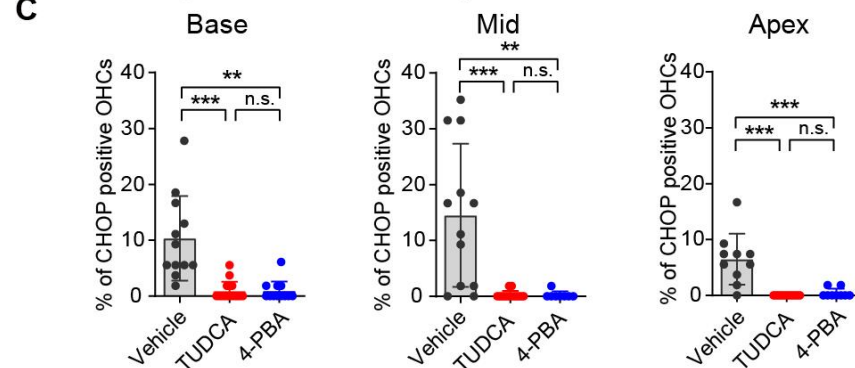
**Figure 22. A strategy for treating noise-induced hearing loss using pharmacological chaperones.** The schedule for intraperitoneal injection of chemical chaperones before and after PTS-induced noise exposure. Injections are once daily up to 2 weeks after noise exposure.



**Figure 23. Pharmacological chaperones have protective effects against hearing loss induced by permanent threshold shift (PTS)-inducing noise exposure.** (A) Auditory brainstem response (ABR) thresholds of mice treated with vehicle (grey), TUDCA (red), or 4-PBA (blue). (B) ABR waveform recordings with the click sound from vehicle and chemical chaperone-treated mice at 2 weeks after PTS-inducing noise exposure. (C) Representative 8 kHz spectra of DPOAE recordings from vehicle- and PERK inhibitor-treated mice. The spectral peaks of the two stimulus tones are labelled as  $f_1$  and  $f_2$ . The measured DPOAE is labelled as  $2f_1-f_2$ . (D) Distortion product otoacoustic emission (DPOAE) thresholds of mice treated with vehicle (grey), TUDCA (red), or 4-PBA (blue). Values and error bars are means  $\pm$  S.E.M. \* $P < 0.05$ , \*\* $P < 0.01$ , \*\*\* $P < 0.001$ , n.s. not significant, two-way ANOVA with Bonferroni's post-hoc analysis.

### **3.7 Pharmacological chaperones suppress the expression of CHOP and aggresomes in hair cells following noise exposure**

Given that PTS-induced noise has been demonstrated to markedly increase CHOP levels and aggresome formation in cochlear hair cells, we investigated whether the pharmacological chaperones' hearing-preserving properties also had an impact on aggresome or CHOP. The expression of CHOP was evaluated in groups treated with TUDCA or 4-PBA compared to the vehicle-treated group after two weeks of exposure to PTS-inducing noise (Figure 24A). In compare OHCs and IHCs to the vehicle-treated group, a significant reduction in CHOP expression was observed across tonotopic regions of the cochlea (Figure 24B and 24C). Furthermore, the expression of aggresomes was examined in the TUDCA or 4-PBA treatment groups after 2 weeks of exposure to PTS-inducing noise. As a result, it was observed that the aggregation staining in the apical region of hair cells decreased in the pharmacological chaperone treatment groups compared to the vehicle-treated group (Figure 25A). In comparison to the vehicle-treated group, there was a significant decrease in the expression of aggresomes in both OHCs and IHCs (Figure 25B and 25B). And no significant difference was observed when compared to the TTS 2-week condition. These findings indicate pharmacological chaperones provide a protective effect against noise-induced hearing loss to decrease the expression of CHOP and aggresomes in OHCs and IHCs of mice exposed to PTS-inducing noise.

**A****B****C**

**Figure 24. Pharmacological chaperones inhibit the expression of CHOP in the hair cells of the cochlea after PTS-inducing noise exposure.** (A) Whole-mount immunostaining of the cochlea from vehicle-treated and pharmacological chaperones, TUDCA and 4-PBA treated mice with Phalloidin (red) and CHOP (green). Scale bars, 30  $\mu$ m. (B-G) Quantitative analysis of CHOP-stained inner (B-D) and outer (E-G) hair cells. The CHOP-positive cells in the 130  $\mu$ m region of the cochlea were counted and quantified as a percentage. Data are expressed as means  $\pm$  SEM. \*P < 0.05, \*\*P < 0.01, \*\*\*P < 0.001, n.s. not significant, one-way ANOVA with Bonferroni's post-hoc analysis.

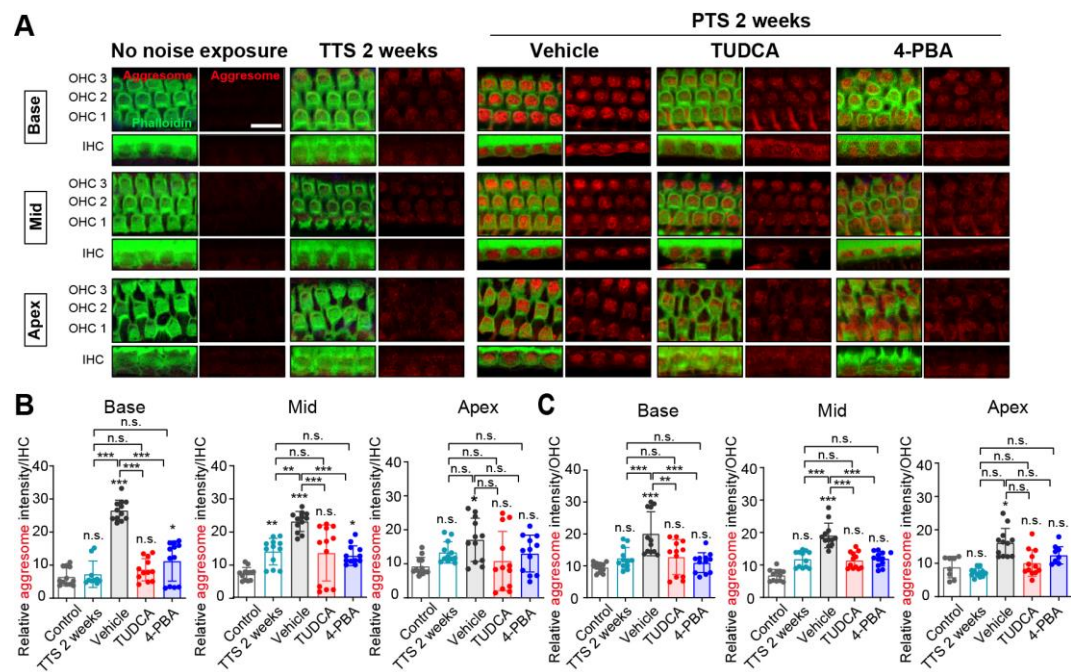


**Figure 25. Pharmacological chaperones inhibit the accumulation of aggresome in the hair cells of the cochlea after PTS-inducing noise exposure.** (A) Whole-mount immunostaining of the cochlea from vehicle-treated and pharmacological chaperones, TUDCA and 4-PBA treated mice including those not exposed to noise and TTS 2 weeks, with Phalloidin (red) and CHOP (green). Scale bars, 30 um. (B-C) Quantitative analysis of aggresomes in inner (B) and outer (C) hair cell. After setting the apical region of each hair cell using phalloidin staining (green), the intensity of aggresomes in the corresponding aggresome image (red) was measured. Scale bar, 10 $\mu$ m. Data are represented as mean  $\pm$  SEM. \*P < 0.05, \*\*P < 0.01, one-way ANOVA with Bonferroni post hoc test.

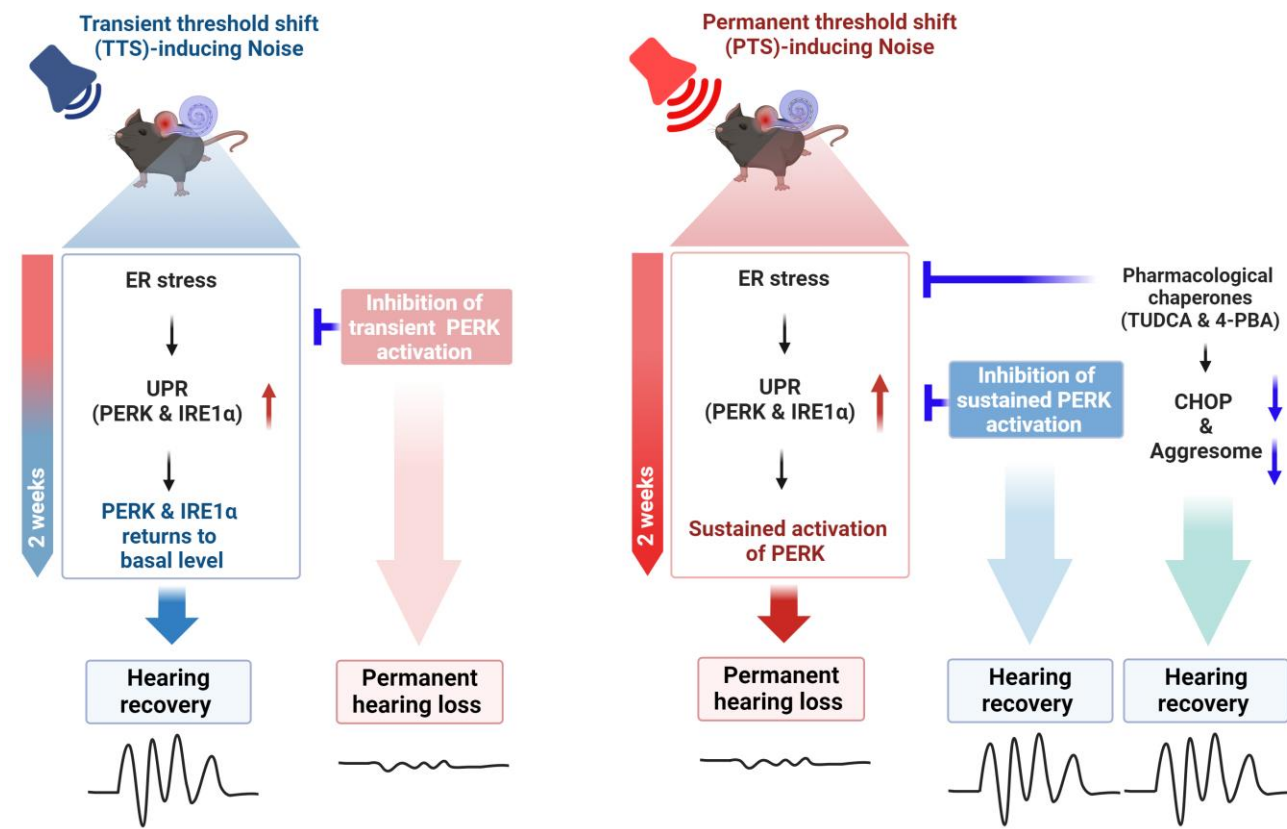


**Figure 26. Graphical summary of unfolded protein response (UPR) activation in the cochlea over time following TTS and PTS-inducing noise exposure.** Unlike TTS, PERK remains continuously activated up to 2 weeks after PTS exposure, and pharmacological chaperones suppress the expression of CHOP and aggresome in hair cells, leading to auditory recovery.

## 4. Discussion

In this study, we investigated changes in cochlear transcriptome at 2 hours, 1 day, and 2 weeks after exposure to TTS- and PTS-inducing noise. We found that exposure to both TTS- and PTS-inducing noise activated ER stress and unfolded protein response. Exposure to TTS-inducing noise activated the PERK and IRE1 $\alpha$  branches of the unfolded protein response (UPR), and at the hearing recovery point of 2 weeks, the levels of PERK and IRE1 $\alpha$  returned to their original expression levels. After exposure to PTS-inducing noise, like TTS, both the PERK and IRE1 $\alpha$  branches were activated. However, after 2 weeks, PERK remained activated, unlike in the case of TTS. The expression of CHOP, a downstream pro-apoptotic factor in the PERK branch, increased significantly in OHCs and IHCs in response to PTS-inducing noise compared to TTS-inducing noise. Furthermore, pharmacological modulation using the PERK inhibitor, GSK2656157, validated the necessity of PERK activation in the hearing recovery process following noise exposure. Our study demonstrates that the administration of pharmacological chaperones such as TUDCA and 4-PBA effectively reduces the expression of CHOP and aggresomes in hair cells induced by PTS-inducing noise, offering protective effects against noise-induced hearing loss. A graphical summary of this mechanism is illustrated in Figure 26.

Currently NIHL requires a proven pharmaceutical intervention. Long-term noise exposure frequently causes irreversible cochlear damage, making medicine useless and emphasizing the value of prevention. So far, numerous studies have investigated the ability of anti-apoptotic and antioxidant agents to prevent hearing loss. Antioxidant treatments like glutathione (GSH)<sup>39-40</sup>, D-methionine<sup>41</sup>, resveratrol<sup>42</sup>, ascorbic acid<sup>43-44</sup>, and water-soluble coenzyme Q10<sup>45</sup> have been shown to reduce hearing loss in animal models when administered before noise exposure. It is also known that NIHL can be prevented by inhibiting apoptotic cascades, such as the MAP kinase (MAPK)-c-Jun-N-terminal kinase (JNK) pathway.<sup>46-49</sup> Additionally, it has been shown that blocking L-type voltage-gated Ca<sup>2+</sup> channels prevent NIHL.<sup>50</sup> However, none of these efforts have demonstrated effects, and the precise mode of action is yet unknown. The Food and Drug Administration (FDA)-approved B-raf inhibitor dabrafenib was identified in a recent study to reduce NIHL without compromising its anticancer properties. However, to reduce the risk of NIHL, this medication is only administered to people who undergo chemotherapy. In this study, we investigated the potential of applying a chemical chaperone as an NIHL treatment. Biliary cirrhosis and urea cycle abnormalities are treated with the chemical chaperones TUDCA and 4-PBA, respectively.<sup>51</sup> FDA-

approved medications TUDCA and 4-PBA have very minor negative effects. TUDCA is also frequently taken as a dietary supplement. Therefore, it is quite straightforward to repurpose these drugs to prevent permanent hearing loss that may occur due to regular or unexpected exposure to loud noises. In our transcriptomic analysis, most of the DEGs exhibited similar expression patterns from the time of noise exposure to hearing recovery in both the TTS and PTS groups. This suggests that noise exposure induces changes in gene expression consistently, but hearing recovery differs between TTS and PTS. Therefore, we hypothesized that signaling pathways exhibiting dual effects on hearing recovery are involved in response to both TTS and PTS-inducing noise. A recent study analyzed cochlear proteomics after noise exposure using two models of noise-induced hearing loss and suggested that protein synthesis may be associated with hearing recovery after noise exposure.<sup>29</sup> However, the mechanisms and therapeutic targets have not yet been fully elucidated. We found that both TTS and PTS-inducing noise exposure activate ER stress and UPR. Particularly, we observed an increase in the expression of CHOP, a downstream signal of PERK, in IHCs after 2 weeks of TTS-inducing noise exposure. While ABR thresholds returned to baseline levels after 2 weeks of TTS-inducing noise exposure, the amplitude of ABR wave I did not return to its original level, indicating hidden hearing loss.<sup>36</sup> The increased expression of CHOP in IHCs after 2 weeks of noise exposure may be one of the factors contributing to hidden hearing loss.

In this study, cell type-specific changes in the cochlea due to each noise exposure were not confirmed through bulk RNA sequencing analysis. In the bulk RNA sequencing analysis, the expression patterns of most genes were similar after TTS and PTS-induced noise exposure, which may be due to the averaging of gene expression across various cell types. Milon *et al.* performed single-cell RNA sequencing 1 day after PTS-induced noise exposure, but specific changes in gene expression upon hearing recovery were not elucidated based on cochlear cell types. Single-cell RNA sequencing enables the identification of gene expression changes at the single-cell level, surpassing bulk RNA-sequencing. However, it loses spatial information during tissue dissociation, which is essential for isolating cells. Moreover, this technique demands significant time, cost, and animal sacrifice during sequencing. Spatial transcriptomics is a technology used to analyze gene expression of individual cells while preserving spatial information in 2D tissue sections. Applying spatial transcriptomics is crucial to accurately identify changes in important cell types with low proportions, such as OHCs and IHCs, within the cochlea. Therefore, further research using spatial transcriptomics is essential to identify specific cell types involved in ER stress and UPR induced by noise and



accurately elucidate signaling pathways related to hearing recovery. Our research findings indicate that the activation of PERK induced by noise exposure is essential for hearing recovery. However, prolonged activation of PERK, as in the case of PTS-induced noise exposure, hinders hearing recovery. Additionally, we observed that long-term inhibition of PERK through treatment with the PERK inhibitor GSK2656157 3 days after PTS-induced noise exposure partially restores hearing. Lastly, our study demonstrates that using chaperones such as TUDCA or 4-PBA to reduce chronic PERK activation can partially reverse hearing loss due to PTS by suppressing the expression of CHOP and aggresomes in OHCs and IHCs.

## 5. Conclusion

The mechanism and therapeutic targets for hearing recovery after noise exposure have not been fully elucidated. This study conducted longitudinal cochlear transcriptome analysis from noise exposure to the period of hearing recovery in two different noise exposure models showing differences in hearing recovery. This research provides new insights into the mechanism of noise-induced hearing loss by demonstrating the following:

- 1 After noise exposure ER stress and UPR, especially the PERK and IRE1A branches, are activated.
- 2 Unlike after TTS-induced noise exposure, the PERK branch remains persistently activated after PTS-induced noise exposure, even at the time of hearing recovery 2 weeks later.
- 3 Initial PERK activation after noise exposure is necessary for hearing recovery, while persistent PERK activation contributes to noise-induced hearing loss.
- 4 Alleviating ER stress caused by noise exposure using pharmacological chaperones has a protective effect against noise-induced hearing loss.

Furthermore, this study may provide key information on longitudinal high-quality cochlear transcriptome data up to the point of hearing recovery and new therapeutic strategies for noise-induced hearing loss.

## REFERENCES

1. Nelson DI, Nelson RY, Concha-Barrientos M, and Fingerhut M. The global burden of occupational noise-induced hearing loss. *Am J Ind Med.* 2005;48(6):446-58.
2. Le TN, Straatman LV, Lea J, and Westerberg B. Current insights in noise-induced hearing loss: a literature review of the underlying mechanism, pathophysiology, asymmetry, and management options. *J Otolaryngol Head Neck Surg.* 2017;46(1):41.
3. Chadha S, Kamenov K, and Cieza A. The world report on hearing, 2021. *Bull World Health Organ.* 2021;99(4):242-A.
4. Raphael Y, and Altschuler RA. Structure and innervation of the cochlea. *Brain Res Bull.* 2003;60(5-6):397-422.
5. Goutman JD, Elgoyhen AB, and Gomez-Casati ME. Cochlear hair cells: The sound-sensing machines. *FEBS Lett.* 2015;589(22):3354-61.
6. Lim R, and Brichta AM. Anatomical and physiological development of the human inner ear. *Hear Res.* 2016;338:9-21.
7. Hudspeth AJ. How the ear's works work. *Nature.* 1989;341(6241):397-404.
8. Yoshioka T, and Sakakibara M. Physical aspects of sensory transduction on seeing, hearing and smelling. *Biophysics (Nagoya-shi).* 2013;9:183-91.
9. McPherson DR. Sensory Hair Cells: An Introduction to Structure and Physiology. *Integr Comp Biol.* 2018;58(2):282-300.
10. Clark WW, and Bohne BA. Effects of noise on hearing. *Jama.* 1999;281(17):1658-9.
11. Ryan AF, Kujawa SG, Hammill T, Le Prell C, and Kil J. Temporary and Permanent Noise-induced Threshold Shifts: A Review of Basic and Clinical Observations. *Otol Neurotol.*

2016;37(8):e271-5.

12. Hertzano R, Lipford EL, and Depireux D. Noise: Acoustic Trauma to the Inner Ear. *Otolaryngol Clin North Am.* 2020;53(4):531-42.
13. Tsuprun V, Schachern PA, Cureoglu S, and Paparella M. Structure of the stereocilia side links and morphology of auditory hair bundle in relation to noise exposure in the chinchilla. *J Neurocytol.* 2003;32(9):1117-28.
14. Hu BH, Guo W, Wang PY, Henderson D, and Jiang SC. Intense noise-induced apoptosis in hair cells of guinea pig cochleae. *Acta Otolaryngol.* 2000;120(1):19-24.
15. Yuan H, Wang X, Hill K, Chen J, Lemasters J, Yang SM, et al. Autophagy attenuates noise-induced hearing loss by reducing oxidative stress. *Antioxid Redox Signal.* 2015;22(15):1308-24.
16. Slepecky N. Overview of mechanical damage to the inner ear: noise as a tool to probe cochlear function. *Hear Res.* 1986;22:307-21.
17. Zheng HW, Chen J, and Sha SH. Receptor-interacting protein kinases modulate noise-induced sensory hair cell death. *Cell Death Dis.* 2014;5(5):e1262.
18. Fujioka M, Okano H, and Ogawa K. Inflammatory and immune responses in the cochlea: potential therapeutic targets for sensorineural hearing loss. *Front Pharmacol.* 2014;5:287.
19. Frye MD, Ryan AF, and Kurabi A. Inflammation associated with noise-induced hearing loss. *J Acoust Soc Am.* 2019;146(5):4020.
20. Bae SH, Yoo JE, Hong JW, Park HR, Noh B, Kim H, et al. LCCL peptide cleavage after noise exposure exacerbates hearing loss and is associated with the monocyte infiltration in the cochlea. *Hear Res.* 2021;412:108378.

21. Ohlemiller KK, and Dugan LL. Elevation of reactive oxygen species following ischemia-reperfusion in mouse cochlea observed in vivo. *Audiol Neurotol*. 1999;4(5):219-28.
22. Yamane H, Nakai Y, Takayama M, Iguchi H, Nakagawa T, and Kojima A. Appearance of free radicals in the guinea pig inner ear after noise-induced acoustic trauma. *Eur Arch Otorhinolaryngol*. 1995;252(8):504-8.
23. Yamashita D, Jiang HY, Schacht J, and Miller JM. Delayed production of free radicals following noise exposure. *Brain Res*. 2004;1019(1-2):201-9.
24. Fridberger A, Flock A, Ulfendahl M, and Flock B. Acoustic overstimulation increases outer hair cell Ca<sup>2+</sup> concentrations and causes dynamic contractions of the hearing organ. *Proc Natl Acad Sci U S A*. 1998;95(12):7127-32.
25. Minami SB, Yamashita D, Schacht J, and Miller JM. Calcineurin activation contributes to noise-induced hearing loss. *J Neurosci Res*. 2004;78(3):383-92.
26. Kim KX, Payne S, Yang-Hood A, Li SZ, Davis B, Carlquist J, et al. Vesicular Glutamatergic Transmission in Noise-Induced Loss and Repair of Cochlear Ribbon Synapses. *J Neurosci*. 2019;39(23):4434-47.
27. Ohinata Y, Miller JM, Altschuler RA, and Schacht J. Intense noise induces formation of vasoactive lipid peroxidation products in the cochlea. *Brain Res*. 2000;878(1-2):163-73.
28. Milon B, Shulman ED, So KS, Cederroth CR, Lipford EL, Sperber M, et al. A cell-type-specific atlas of the inner ear transcriptional response to acoustic trauma. *Cell Rep*. 2021;36(13):109758.
29. Jongkamonwiwat N, Ramirez MA, Edassery S, Wong ACY, Yu J, Abbott T, et al. Noise Exposures Causing Hearing Loss Generate Proteotoxic Stress and Activate the Proteostasis Network. *Cell Rep*. 2020;33(8):108431.

30. Ohlemiller KK, Wright JS, and Dugan LL. Early elevation of cochlear reactive oxygen species following noise exposure. *Audiol Neurotol*. 1999;4(5):229-36.
31. Kurioka T, Matsunobu T, Satoh Y, Niwa K, Endo S, Fujioka M, et al. ERK2 mediates inner hair cell survival and decreases susceptibility to noise-induced hearing loss. *Sci Rep*. 2015;5:16839.
32. Xue Q, Li C, Chen J, Guo H, Li D, and Wu X. The Protective effect of the endoplasmic reticulum stress-related factors BiP/GRP78 and CHOP/Gadd153 on noise-induced hearing loss in guinea pigs. *Noise Health*. 2016;18(84):247-55.
33. Cai Q, Vethanayagam RR, Yang S, Bard J, Jamison J, Cartwright D, et al. Molecular profile of cochlear immunity in the resident cells of the organ of Corti. *J Neuroinflammation*. 2014;11:173.
34. Liewluck T, Hayashi YK, Ohsawa M, Kurokawa R, Fujita M, Noguchi S, et al. Unfolded protein response and aggresome formation in hereditary reducing-body myopathy. *Muscle Nerve*. 2007;35(3):322-6.
35. Freeman S, Mateo Sánchez S, Pouyo R, Van Lerberghe PB, Hanon K, Thelen N, et al. Proteostasis is essential during cochlear development for neuron survival and hair cell polarity. *EMBO Rep*. 2019;20(9):e47097.
36. Hetz C. The unfolded protein response: controlling cell fate decisions under ER stress and beyond. *Nat Rev Mol Cell Biol*. 2012;13(2):89-102.
37. Woehlbier U, and Hetz C. Modulating stress responses by the UPRosome: a matter of life and death. *Trends Biochem Sci*. 2011;36(6):329-37.
38. Read A, and Schröder M. The Unfolded Protein Response: An Overview. *Biology (Basel)*. 2021;10(5).

39. Yamasoba T, Harris C, Shoji F, Lee RJ, Nuttall AL, and Miller JM. Influence of intense sound exposure on glutathione synthesis in the cochlea. *Brain Res.* 1998;804(1):72-8.
40. Ohinata Y, Yamasoba T, Schacht J, and Miller JM. Glutathione limits noise-induced hearing loss. *Hear Res.* 2000;146(1-2):28-34.
41. Campbell KC, Meech RP, Klemens JJ, Gerberi MT, Dyrstad SS, Larsen DL, et al. Prevention of noise- and drug-induced hearing loss with D-methionine. *Hear Res.* 2007;226(1-2):92-103.
42. Seidman M, Babu S, Tang W, Naem E, and Quirk WS. Effects of resveratrol on acoustic trauma. *Otolaryngol Head Neck Surg.* 2003;129(5):463-70.
43. McFadden SL, Woo JM, Michalak N, and Ding D. Dietary vitamin C supplementation reduces noise-induced hearing loss in guinea pigs. *Hear Res.* 2005;202(1-2):200-8.
44. Heinrich UR, Fischer I, Brieger J, Rümelin A, Schmidtmann I, Li H, et al. Ascorbic acid reduces noise-induced nitric oxide production in the guinea pig ear. *Laryngoscope.* 2008;118(5):837-42.
45. Fetoni AR, Piacentini R, Fiorita A, Paludetti G, and Troiani D. Water-soluble Coenzyme Q10 formulation (Q-ter) promotes outer hair cell survival in a guinea pig model of noise induced hearing loss (NIHL). *Brain Res.* 2009;1257:108-16.
46. Wang J, Van De Water TR, Bonny C, de Ribaupierre F, Puel JL, and Zine A. A peptide inhibitor of c-Jun N-terminal kinase protects against both aminoglycoside and acoustic trauma-induced auditory hair cell death and hearing loss. *J Neurosci.* 2003;23(24):8596-607.
47. Wang J, Ruel J, Ladrech S, Bonny C, van de Water TR, and Puel JL. Inhibition of the c-Jun N-terminal kinase-mediated mitochondrial cell death pathway restores auditory

function in sound-exposed animals. *Mol Pharmacol.* 2007;71(3):654-66.

48. Shim HJ, Kang HH, Ahn JH, and Chung JW. Retinoic acid applied after noise exposure can recover the noise-induced hearing loss in mice. *Acta Otolaryngol.* 2009;129(3):233-8.
49. Ahn JH, Kang HH, Kim YJ, and Chung JW. Anti-apoptotic role of retinoic acid in the inner ear of noise-exposed mice. *Biochem Biophys Res Commun.* 2005;335(2):485-90.
50. Uemaetomari I, Tabuchi K, Nakamagoe M, Tanaka S, Murashita H, and Hara A. L-type voltage-gated calcium channel is involved in the pathogenesis of acoustic injury in the cochlea. *Tohoku J Exp Med.* 2009;218(1):41-7.
51. Ozcan L, Ergin AS, Lu A, Chung J, Sarkar S, Nie D, et al. Endoplasmic reticulum stress plays a central role in development of leptin resistance. *Cell Metab.* 2009;9(1):35-51.

## Abstract in Korean

### 소음성 난청에서 펼쳐진 단백질 반응의 역할 및 치료적 타겟 탐색

소음으로 인한 청력 손실은 소음 노출 강도와 기간에 따라 일시적 (일시적 청력 역치 이동, TTS) 또는 영구적 (영구적 청력 역치 이동, PTS)일 수 있다. 과도한 소음에 장기간 노출되면 산화 스트레스, 면역 반응, 세포사멸 등 달팽이관 내 다양한 세포 메커니즘이 활성화된다. 그러나, 현재까지 TTS 및 PTS 유도 소음에 노출된 직후부터 청력 회복 시점까지의 달팽이관 전사체에 대한 종단연구는 진행된 바가 없었다. 우리는 두 가지 서로 다른 조건의 소음에 노출된 성인 쥐의 달팽이관 전사체의 시간의 흐름에 따른 변화를 분석하여 소음성 난청의 메커니즘 및 치료적 타겟을 조사했다. 우리는 소음 노출에 의해 유발된 소포체 스트레스가 펼쳐진 단백질 반응 (UPR)을 활성화하고, 특히 UPR 경로 중 IRE1 $\alpha$ 와 PERK를 활성화한다는 것을 발견했다. 또한 PERK 경로는 소음 노출 후 최대 2주까지 PTS 유도 소음 노출에 의해 지속적으로 활성화되었지만 TTS 유발 소음 노출에 의해서는 청력 회복 시점에 원래 발현 수준으로 돌아왔다. PERK 경로의 하위 인자인 세포사멸 촉진 인자 CHOP는 PTS 소음 노출에 의해 외유모 및 내유모 세포에서 모두 유의하게 발현이 유도되었다. 그러나, 소음 노출 전 PERK 억제제를 사용한 치료는 청력을 회복하지 못했으며 이는 청력 회복을 위해 PERK 활성화가 필요함을 의미한다. 흥미롭게도 TUDCA (타우로르소데옥시콜산) 및 4-PBA (4-페닐부티르산)와 같은 약리학적 샤페론 치료는 소음으로 인한 청력 상실에 보호 효과를 나타냈다. 종합적으로, 소음성 난청 메커니즘에 미접힘 단백질 반응 중 PERK 경로가 밀접한 연관이 있으며 소음 노출 후 청력을 회복하기 위해 초기 활성화가 필요하며 지속적인 활성화는 청력 회복을 방해하는 역할을 수행하고 있음을 시사한다. 또한, 약리학적 샤페론을 이용한 소음성난청에서의 청력 회복 효과는 기존에 알려져 있지 않았던 소음성 난청에서의 새로운 치료적 타겟 가능성을 제시한다.

---

핵심되는 말 : 소음성난청; RNA 시퀀싱; 소포체 스트레스; 미접힘 단백질 반응; PERK; CHOP; 약리학적 샤페론; TUDCA; 4-PBA